

Screen-Printed Technologies Combined with Flow Analysis Techniques: Moving from Benchtop to Everywhere

Nathália Florência Barros Azeredo,* Mauro S. Ferreira Santos, Juliane R. Sempionatto, Joseph Wang, and Lúcio Angnes*



Cite This: *Anal. Chem.* 2022, 94, 250–268



Read Online

ACCESS |

Metrics & More

Article Recommendations

ABSTRACT: Screen-printed electrodes (SPEs) coupled with flow systems have been reported in recent decades for an ever-growing number of applications in modern electroanalysis, aiming for portable methodologies. The information acquired through this combination can be attractive for future users with basic knowledge, especially due to the increased measurement throughput, reduction in reagent consumption and minimal waste generation. The trends and possibilities of this set rely on the synergistic behavior that maximizes both SPE and flow analyses characteristics, allowing mass production and automation. This overview addresses an in-depth update about the scope of samples, target analytes, and analytical throughput (injections per hour, limits of detection, linear range, etc.) obtained by coupling injection techniques (FIA, SIA, and BIA) with SPE-based electrochemical detection.

1. INTRODUCTION

Portable assays represent a major recent trend in analytical chemistry, ranging from *in situ* environmental analysis to point-of-care applications. In order to meet the ever-growing demand and the needs of specific assays, the development of portable devices has been pushed toward fast response, low cost, simplicity (user-friendly), and high accuracy.^{1,2} In this context, electrochemical techniques have attracted increasing interest due to easy miniaturization and compliance with several of the requirements for *in situ* measurements.³ Nowadays, many portable instruments are commercially available, including hand-held potentiostats, along with screen-printed electrodes (SPEs) with working electrodes made of conventional materials (e.g., gold, graphite, palladium, platinum, silver) or containing different modifiers (e.g., graphene, single and multiwalled carbon nanotubes, Prussian Blue).⁴ SPEs are compatible with a variety of electrochemical cells available for batch and flow systems, as well as devices for single-drop measurements ($\sim 50 \mu\text{L}$).⁵ Furthermore, the development of new films and materials will increase the scope of applications and the quality of SPEs.⁶

The combination of electrochemical techniques such as voltammetry and amperometry with flow or batch injection analysis methods has been widely explored to improve sample throughput (analytical frequency), automation, repeatability, sensitivity and selectivity, and sample handling capabilities as well as to minimize waste generation and the cost of instrumentation. They are based on the injection of a discrete aliquot of sample into a carrier stream, where the sample can be either carried without undergoing chemical reactions or processed before reaching the electrode.^{7–9}

Flow injection analysis (FIA) is the most disseminated among the injection analysis methods. Since its introduction in

1974,⁸ FIA has gained popularity especially due to the simplicity of experimental setups. Sequential injection analysis (SIA) was introduced in 1990, and it is considered the next generation of FIA.¹⁰ SIA is centered on a multiple port valve, which allows precise handling of samples and reagents, favoring operations that involve complex chemical reactions.¹¹ Besides that, it can be coupled to different detectors without reconfiguration of the flow manifold. Batch injection analysis (BIA) was introduced in 1991 and is the simplest injection analysis technique¹² on which the main component is an automated pipette, and it can be very favorable for routine analysis. In this Review, we present a critical evaluation on the progress of injection analysis techniques combined with SPEs. This combination is an active research topic and has been covered in many scientific articles. Review papers on FIA,^{13,14} SIA,¹⁴ BIA,¹⁵ and SPEs^{9,16} can be found in the literature separately as themes. According to our knowledge, only a brief review, focusing on the recent advancements (last 5 years), has covered the combination of all flow injection techniques and SPEs.¹⁷

In this manuscript, we aimed to address the fundamentals and practical aspects of each technique. Therefore, we reviewed all of the most relevant available papers associating SPEs and flow systems, from the starting point of the techniques throughout December 2020. We also highlighted the key advances in portable instruments and capabilities for *in*

Special Issue: Fundamental and Applied Reviews in Analytical Chemistry 2022

Published: December 1, 2021



situ applications, including miniaturization and battery-powered devices. A timeline covering the past decades of combined injection and programmed flow in the designing of new SPE is presented (Figure 1) alongside with future insights and perspectives discussions.

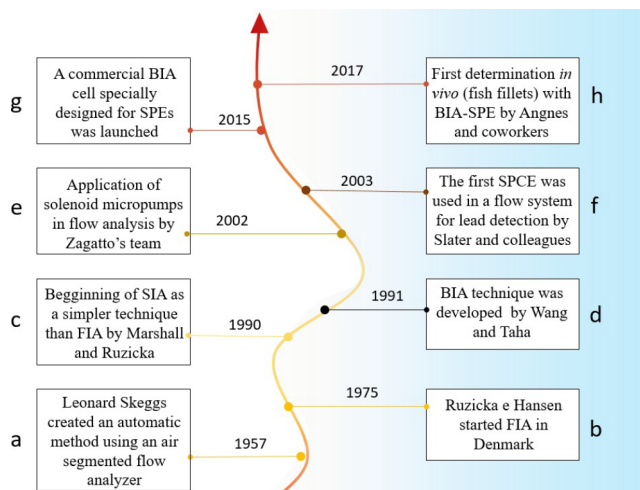


Figure 1. An overview of the “flow injection” techniques (FIA, BIA, SIA) timeline.

2. SCREEN PRINTED ELECTRODES (SPES)

Historically, the screen-printing technique was created to transfer ink to the surface of tissues in desired regions.⁷ Many authors attribute its origin to China, where colored tissues about 2000 years old were found.⁹ The earliest stencils known were produced by the Sung Dynasty (A.C. 960–1280). Basically, screen printing is the process of passing ink through a stencil mesh screen to create a printed design.¹⁶ The process is sometimes called serigraphy or silkscreen printing, but they all refer to the same basic method used to produce SPES (screen printed electrodes).¹⁷

Screen-printed techniques have been used with great success in the manufacture of SPES in the past three decades. The need for a self-monitoring device was the crucial driving force for the

development of the SPES. A schematic representation of the screen-printing process is shown in Figure 2.¹⁸

Screen-printing allows mass production of electrodes at an extremely low cost; it is simple and can be performed in any laboratory, being suitable for the production of numerous disposable electrodes in a relatively short amount of time.⁷ The SPE consists of a conductive film deposited on an inert support, usually PVC or alumina ceramic. In general, this conductive film is partially covered (in its middle region) by a second layer of an insulator. In this way, in one extremity is defined the electrode area, and on the opposite side remains the conductive material to establish the electrical contact with the potentiostat.⁵

One of the main aspects for the popularity of SPES is the automation of the manufacturing process to build the complete cell arrangement, constituted by working, counter, and reference electrodes, all of them printed on the same support.⁹ Nowadays, the reliability of these sensors is growing, making this kind of device extremely attractive. In recent years, companies have developed skills to construct (and sell) reproducible electrodes. The first SPES were prepared with conductive inks, exploring the well-known technology previously used in the electronic area. Carbon ink is the most used material, perhaps due to the knowledge of its electrochemical characteristics and also due to the price of its pastes. Gold, silver, platinum, and palladium have also been often used.⁴

Rapidly, researchers started to utilize the commercial carbon SPES to deposit bismuth (Bi) films, in order to produce electrodes for stripping analysis, using the deposition of Bi and (trace) metals to be quantified simultaneously¹⁹ or making the deposition of Bi *ex situ*, followed by the quantification of heavy metals in the sample.²⁰ This trend led to the appearance of commercial SPES containing films or nanocomposites of different metals, including bismuth, nickel, antimony, chromium, tin, aluminum, lead, tantalum, tungsten, and cobalt.^{16,17}

The electrode manufacturers quickly detected a huge range of options beyond carbon electrodes and noble metals. The electrode modification opened the possibility to create almost an infinite arsenal of different sensors. Currently, electrodes containing other forms of carbon (graphene, reduced and oxidized graphene, multi- and single walled carbon nanotubes,

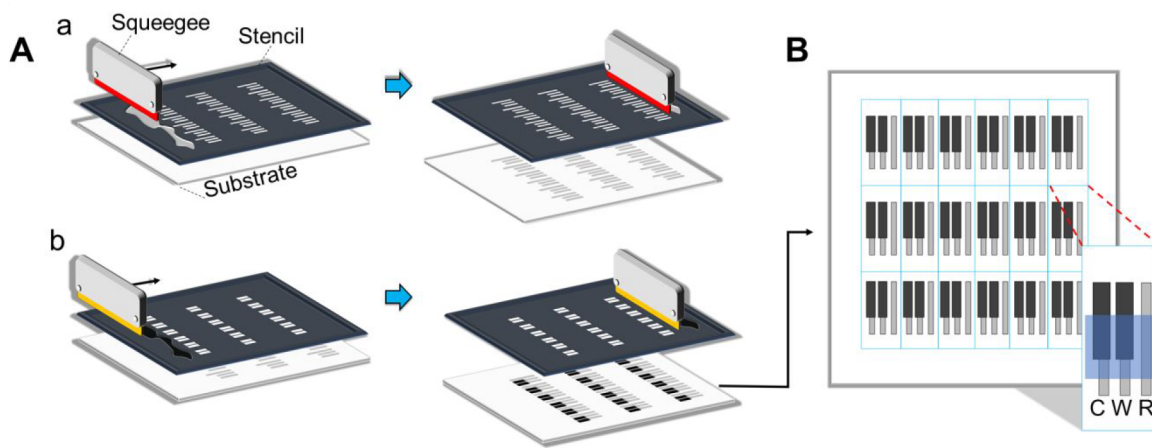


Figure 2. (A) Schematic illustration of the screen-printing process on a substrate using a stencil containing the electrode design and a squeegee. (a) Screen printing the conductive current collector traces and reference electrode. For this step, Ag/AgCl ink is usually used. (b) Screen printing the working and counter electrode over the current collector traces. For this step, a carbon-based ink is usually used. (B) Resulting printed electrodes.

boron-doped diamond electrodes, carbon nanofibers, mesoporous carbon), noble metal particles (palladium, gold, platinum, rhodium, iridium), and metal oxides (bismuth oxide, nickel oxide) are commercially available. Electrodes modified by simple organic species, porphyrins, or mediators are other examples of SPE modification nowadays.

The modification of the SPE with two or more constituents can produce electrodes with great synergy for many applications. These are the cases of electrodes containing carbon nanotubes, carbon nanofibers, or graphene associated with gold nanoparticles (Au-NPs). SPEs associating ferrocyanide and enzymes have been sold as potentiometric and selective biosensors. There are also transparent SPEs (ITO, PEDOT, gold optically transparent or carbon optically transparent) with great potential for spectro-electrochemical experiments, electrodes with quantum dots, and streptavidin. Arrangements with 4, 8, and 96 electrodes are commercialized, and the companies also provide customized SPEs.²¹

All of these possibilities are just a bright start, associated with the simplicity of preparation and the variety of modifying species for the surface of the working electrode. There are also other opportunities to develop potentiometric and ion-selective SPEs, molecularly imprinted sensors, SPEs with nanoparticles (NPs), SPEs modified with immunosensors, DNA, RNA, etc. These features promise to place SPEs in a privileged position among other sensors.¹⁶

The manufacturing process of SPEs is supported by a number of printing technologies that have been developed to design a wide range of electronic materials using different substrates. These studies are also of great importance for the development of electrodes with larger sizes and great flexibility for applications in wearable devices.²² The main printing technologies can be classified as contact, noncontact, and roll-to-roll printing according to the need for manufacturing electronic devices.

Initially, SPEs were predominantly manufactured via a screen-printing process. More recently, the use of inkjet printing has received great attention from the scientific community. The quality of the manufactured electrode will depend on the careful selection of the materials and processes. A brief description of some factors to be considered are as follows,

a. Substrate. The characteristics of the substrate play an important role in the performance of the electrode, once it can affect the stickiness of its surface. Although polymeric materials such as polyethylene terephthalate (PET), polyethylene naphthalene (PEN) polyimide (PI), and polyurethane (PU) are widely used in the electronic field, ceramic substrate²⁴ has been the material of choice for SPE suppliers, especially due to its inertness and tolerance for thermal curing. The use of polymeric materials (e.g., PET) has attracted the attention of companies due their lower cost, easy availability, and flexibility.^{23,25}

b. Inks. The composition of inks is the key for the success of an SPE, and at least three components are definitely essential: a conducting filler, a nonconducting binder, and a volatile solvent. After printing, the solvent evaporates, leaving the filler and the binder fixed on the substrate. Ideally, these two components should be uniformly distributed in the mixture, to ensure a close contact of all the conducting particles on the filler, favoring the electron tunneling along the electrode. According to some authors,²⁶ 1.4 nm is the maximum distance between particles for electron tunneling

to occur. Some calculations showed that to attain optimum conditions, the percentage of the filler should be larger than 64%.

Over the years, numerous combinations of binder and solvent were examined for screen printed applications. However, only thermosetting and thermoplastic are preferred as polymeric binders. In several cases, SPEs receive other constituents in their compositions, such as additives and plasticizers, but the content of binder should be well controlled, once all of them impact the electrode conductivity.

c. Additional Aspects. The compatibility between the substrate and the ink is a very important aspect to be considered. Additionally, the rheological/fluidic characteristics of the ink in different printing systems will dictate the aspects relative to storage conditions, formulation, and quality of final films.²⁴ The surface tension of any prepared ink is also dependent on the solvent used and other constituents. Such tension can be significantly altered simply by the addition of a very small quantity of polar or nonpolar surfactants to the ink. Finally, the contact angle provides information about the interactions between the ink and the surface of the substrate. Inks that do not spread well on the surface (form high contact angles) indicate poor wetting properties, and this is not adequate for printing applications.

3. FLOW INJECTION ANALYSIS (FIA)

Flow injection analysis (FIA) consists of injecting a well-defined sample zone into a carrier stream, which may contain reagents that will react (or not) with the sample to be analyzed. The product of this reaction is carried to the detector, which will produce a signal proportional to the concentration of the analyte. The automation of FIA systems speeds up the analytical processes, increasing the reproducibility compared to the manual method previously used. In principle, each measurement starts by aspirating a wash solution, followed by sample injection, and both are conducted to the detection zone.¹³ In the flowing stream, the sample can react during the transport process and suffers dilution before reaching the detector. Reactions during the transport of the analyte are usually employed for spectrophotometric measurements. In the case of voltammetric (or amperometric) detection, these reactions are rarely explored. It allows the detector to be positioned closer to the injection valve to reduce the dilution of the analyte.¹⁷

FIA changed significantly the way to perform chemical analysis due to the mechanization of analytical procedures in a continuous flowing stream, allowing the use of unstable reagents and/or measurement of unstable products. The principles and applications of this methodology are recorded in many books, several theses, and thousands of papers. Processes such as chemical derivatization, separations, complexations, redox reaction, analyte concentration, and controlled dilutions have been efficiently carried out under reproducible FIA conditions. Since the samples are handled in a closed system, risks of sample contamination by the analyst are diminished.¹⁴

A schematic representation of a conventional flow cell for SPEs that can be used in FIA and SIA systems is shown in Figure 3A. The most common approach is the wall-jet configuration where the inlet flow reaches the working electrode in a 90° angle. It increases the mass transport and therefore the signal intensity as well as reduces the cleaning time that leads to a higher analytical frequency. A schematic

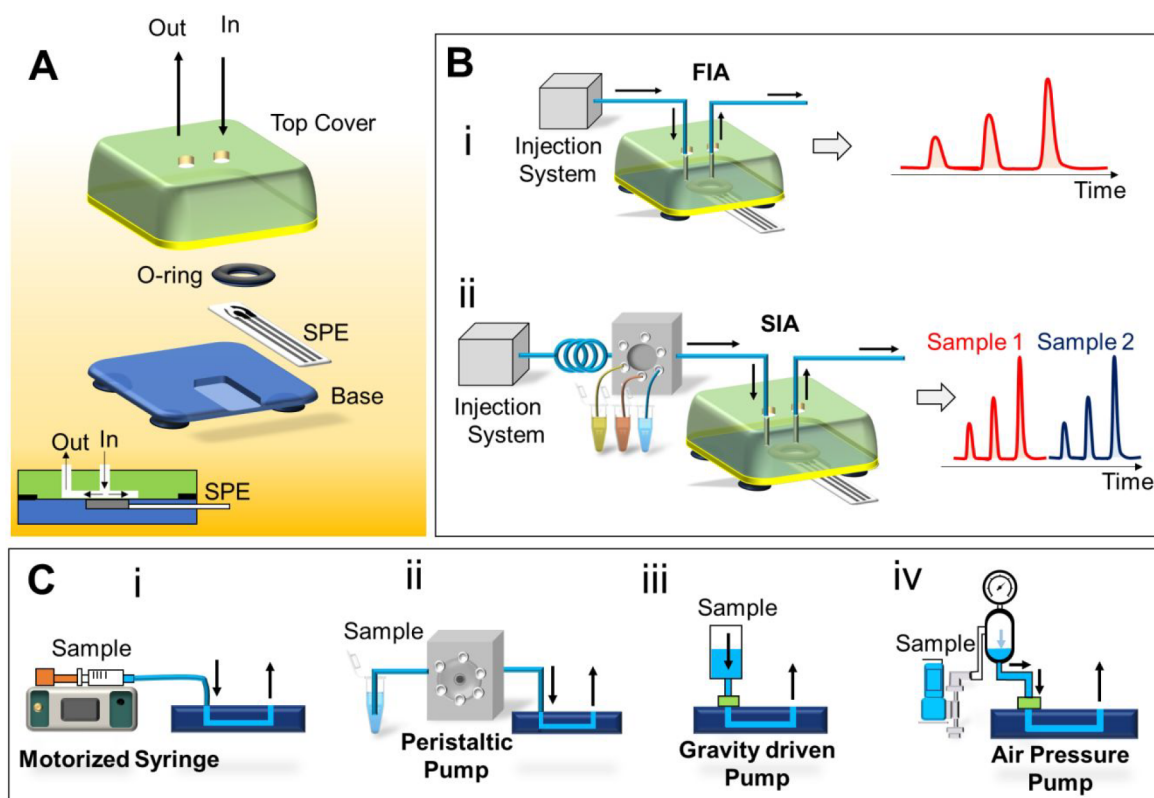


Figure 3. (A) Schematic illustration of the flow cells used in FIA and SIA systems. (B) Illustration of the basic working principle of (i) FIA and (ii) SIA systems. The sample is introduced into the flow stream using an injector (left) and the corresponding signal recorded over time (right). (C) Examples of mechanisms for continuous flow in FIA or SIA analysis. (i) Motorized syringe, (ii) peristaltic pump, (iii) gravity driven pump, and (iv) air pressure pump.

representation of FIA and SIA setups with the corresponding measured signal is shown in Figure 3B. Various mechanisms to provide a continuous flow for FIA or SIA analysis are shown in Figure 3C.

3.1. Screen-Printed Electrodes (SPE) Associated with FIA. Screen-printed carbon electrodes (SPCE) are one of the most popular electrodes utilized in association with FIA. In addition to the wide electrochemical window of these electrodes, this preference may be a result of low-cost materials and simple procedures to produce “carbon inks” as well as the availability of commercial SPCEs at attractive prices. Other forms of SPEs (carbon, metallic films, deposition of nanomaterials, and immobilization of enzymes) will be also discussed in the next sections. Manuscripts were carefully reviewed, and a selected set is described in more detail in this section, while the complete list of manuscripts is summarized in Table 1. Some relevant works on the FIA and SPE association are highlighted in Figure 4.

3.1.1. Unmodified Screen-Printed Carbon Electrodes (SPCE). Screen-printed carbon electrodes are the simplest (and the cheapest) among SPEs and have been used in a variety of applications related to safety,³¹ environmental,³² pharmaceutical,^{33–35} and food^{28,36–38} analysis.

The use of SPCEs for the determination of pharmaceuticals such as procaine was reported, and the method presented an analytical frequency of 36 injections per hour.³³ A preanodized SPCE was employed for the detection of Isoniazid (INZ) in a neutral medium and a detailed surface characterization (X-ray and Raman spectroscopy) study of the electrode indicated that both the edge/defects’ sites and the oxygen functionalities

favor the INZ oxidation.³⁵ Although amperometry has been the most used technique in FIA-SPE combination, adsorptive stripping voltammetry (ASV) was explored for preconcentration of nifuroxazide and its determination in pharmaceutical formulations.³⁴

A microfluidic electroanalytical device using 3D printed structures and cotton threads as microchannels was employed in the amperometric determination of gallic and caffeic acids in wine samples.³⁶ Both analytes presented a linear response applying SPCE in the range of 5.0×10^{-6} to 1.0×10^{-3} mol L⁻¹ and limit of detection (LOD) of 1.5×10^{-6} and 8.0×10^{-7} mol L⁻¹, respectively. The electrochemical behavior of ethoxyquin (a food preservative) and the effect of the products generated during the oxidation process were investigated in an FIA cell with dual SPCE.³⁷ Linear responses in the 20–100 μ mol range and an LOD of 7.5 μ mol were obtained in the quantification of ethoxyquin in salmon samples. The combination of FIA and liquid chromatography with electrochemical detection was explored for quantification of the antibiotic lincomycin in urine and foodstuffs.³⁸ A preanodized SPCE was used associated with solid-phase extraction aiming at a fast-screening assay. Since the preanodized SPCE holds the advantages of low cost and easy handling, the proposed approach offers a good possibility for use in routine analysis of lincomycin.

A customized FIA electrochemical cell coupled to an SPCE (Figure 4B) was utilized to evaluate the effect of temperature on the electrooxidation of ascorbic acid.²⁸ A light beam was used to heat the SPCE without decomposing the substrate. The observed enhancement in the electrooxidation process

Table 1. Studies Involving Screen-Printed Electrodes (SPE) Associated to FIA^a

electrode material	analyte	sample (matrix)	linear range ($\mu\text{mol/L}$)	LOD ($\mu\text{mol/L}$)	flow rate ($\mu\text{L/min}$)	ref
SPCE	procaine	pharmaceuticals	9.0–100	6.0	3800	33
SPCE	gallic and caffeic acid	wine	5.0–1000	1.5 and 0.8	43	36
dual–SPCE	ethoxyquin	salmon	20–100	7.5	100	37
nanofiber – SPCE	nifuroxazide	pharmaceuticals	0.1–3 ($\mu\text{g/mL}$)	42 (ng/mL)	1500	34
SPCE	ascorbic acid	orange juice		0.0287	400	28
ring–disk SPE	arsenite	tap water	up to 10	0.07	400	32
preanodized ring–disk SPE	zinc phenolsulfonate	cosmetic	0.1 to 5 (mg/L)	76 (ppb)	600	27
preanodized SPCE	INZ	human urine	0.01–1000	0.0027	800	35
preanodized SPCE	lincomycin	feeds, honey, milk, and urine	up to 1000	0.08	400	38
SPCE	H ₂ O ₂	PBS	up to 10000	1000	1000	29
SPCE	glucose	blood	up to 1200		800	39
SPCE	<i>Salmonella typhimurium</i>	milk	10–0*100 cells/mL	7.7 cells/mL	100	31
SPCE	tumor biomarkers	Britton–Robinson buffer (pH = 2)	0.05–100	0.012–0.065	1000	40
SPE–CNT	paracetamol	pharmaceuticals	2.5–1000	0.1	2000	41
SPE–CNT	paracetamol, naproxen	pharmaceuticals	10–800 and 10–400	0.4 and 0.3	2500	42
SPCE	estriol hormone	pharmaceutical	1.0–1000	0.53	30	43
SPE	NPs	alcohol fuel cells			1000	49
SPCE	H ₂ O ₂	disinfectant, hair colorant, and milk	100–1000	20	1300	46
SPE–CNF	nitrofurantoin	urine	19.1 to 76.2 (ng/mL)	3.8 (ng/mL)		47
SPE–CNT	hydroquinone	water	1–50	0.1	1000	48
SPE–CNF	nimodipine	pharmaceuticals	0.08 to 0.400	0.08 to 0.4		44
SPE–CNF	nitrofurantoin, furazolidone, nitrofurazone	chicken muscle	0.1–8.0	0.016, 0.015, 0.034	1330	45
SPCE	fenobucarb	vegetables	0.025–110	0.0089	1200	30
gold–sputtered SPCE	lead	spiked drinking and tap water	0–50 ($\mu\text{g/L}$)	0.8 ($\mu\text{g/L}$)	1080	50
SPAuE	nitromethane	vapor	0.7–8.2 (ppm)	4.5	3500	51
SPCE–Ag–NC	nitrite	meat products	2.0–800	4.5	2000	54
SPAuE	aluminum chlorohydrate	antiperspirants	1–200 (ppm)	295 ppb	500	53
SPCE	bromate	hair waving products	66–2000	0.0232	1000	55
SPE/Ni/Cu	glucose	beverages	up to 1000	0.33	2500	56
SPE	cadmium	mineral water and seawater	up to 60 ($\mu\text{g/L}$)	0.79 ($\mu\text{g/L}$)	700	57
dual–SPAuE	tryptophan and pyridoxine	pharmaceutical	0.5–5000 and 0.05–5000		2150	52
SPCE	INZ	human urine	5.0–500	2.6	2900	58
CNF–chitosan SPE	INZ	pharmaceuticals	1–1000	0.172	800	59
SPCE	zinc pyrithione	hair care products	6–576	0.9	400	60
SPAuE	2-nitro-p-phenylenediamine	hair dyes	4.3–22.5	1.2 and 1.6	1120	61
SPE carbon black NPs	phosphates	water	up to 500	6	500	62
SPAuE	urinary 3-hydroxyanthranilic acid	urine	50–550 (ng/mL)	3.06 (pg/mL)		65
SPCE	chromium(VI)	water	0.1–10 (mg/L)	0.097 (mg/L)		64
SPCE	chlorine	water	7.5–3000 (ppb)	8.25 (ppb)	2500	63
SPE	mainly gallic acid	green tea	up to 500	0.15	800	66
MnO ₂ –GOx–SPE	glucose	beer	11–13.900	1	200	68
CuO–graphene SPCE	glucose	0.1 M NaOH	0.122–500	0.0343	600	72
Fe ₃ O ₄ @Au/SPCE MnO ₂	glucose	food and drinks	200–9000	100	1700	69
Os–complex SPE	glucose	0.2 M phosphate buffer	500–30000		800	70
Meldola's Blue Reinecke salt–SPCE	glucose	serum	75–30000		800	71
AChE–Al ₂ O ₃ –SPE	organophosphorus pesticide	seawater and distilled water	0.1–80 and 1–60	0.08 and 0.8	347	73
CNT–SPCE	organophosphorus	rat saliva			200	76
AChE–SPE	chlorpyrifos-oxon and malaoxon	milk	0.0005–0.000005 and 0.0001–0.00009	0.000005 and 0.00005	500	77
magnetic beads–SPE	organophosphate	water	10 ^{–3} to 10 ^{–4}	0.000043	300	74
Prussian Blue NPs–SPE	organophosphorus	water	0.007–0.04	0.004	120	75
SPCEs	H ₂ O ₂ and phenolic compounds	20 mM phosphate buffer (pH 6.0)	0.5–500, 0.5–250, and 1–250	0.40, 0.48, and 0.98	225	78
AuNPs SPE	gallic acid	wines	30–300	6.0	894	79

Table 1. continued

electrode material	analyte	sample (matrix)	linear range ($\mu\text{mol/L}$)	LOD ($\mu\text{mol/L}$)	flow rate ($\mu\text{L/min}$)	ref
AuNPs–CNT–SPCE	phenol	tap water	0.01–0.2	0.0029	26.4	80
graphene–SPCE	acetaminophen	urine	up to 130	1.1	600	81
thionine SPCE	NADH	phosphate buffer (pH 6.9)	5–100	3.0	500	82
azure A and toluidine modified SPCE	NADH	phosphate buffer (pH 6.9)	5–100	0.2 and 0.32	750	83
Meldola's Blue Reinecke salt–SPCE	lactate	serum (pH = 10)	250–10000		800	84
immuno-electrode–SPCE	antigen	mouse IgG as a model analyte	30–700 ng mL ⁻¹	3 ng mL ⁻¹	200	85
magnetic beads–SPE	biotin	pharmaceuticals	0.00001–0.001	0.0000075	1000	86
magnetic beads–SPCE	ochratoxin A	beer	0.1–1 ($\mu\text{g/L}$)	0.06 ($\mu\text{g/L}$)	96	87
iridium oxide NPs–SPE	methimazole	serum and pharmaceuticals	0.01–0.5	0.003	50	88
graphite–prussian blue–SPE	uric acid	urine	10–200	3.0	2100	89
graphene–chitosan–prussian blue–SPCE	uric acid	human blood sérum	2.5 and 400	2.5	300	90

^aAu NPs, gold nanoparticles; CNF, carbon nanofibers; CNT, carbon nanotubes. E_{disc} and E_{ring} are the potentials applied to the disc (generator) and ring (collector) electrodes of a disc-ring electrode, respectively. INZ, Isoniazid; LOD, limit of detection; NPs, Nanoparticles; SPAGe, screen-printed silver electrode; SPAuE, screen-printed gold electrode; SPCE, screen-printed carbon electrode; SPE, screen-printed electrode; SPE-CNF, carbon nanofibers screen printed electrode; SPE-CNT, carbon nanotubes screen printed electrode.

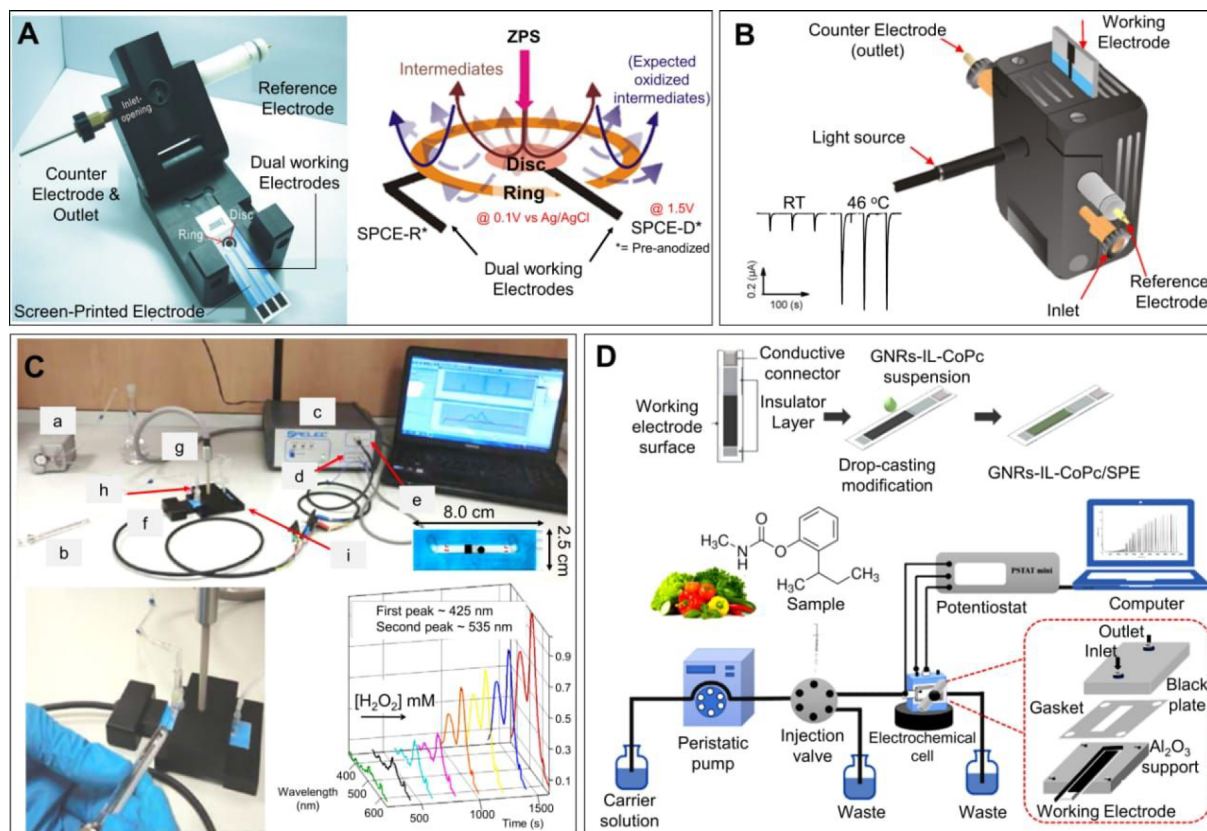


Figure 4. Examples of SPE-FIA applications. (A) Disposable screen-printed carbon ring-disc electrode (SPCE-D*/R* = preanodized) coupled with FIA and its application in the electrochemical detection of zinc phenolsulfonate (ZPS). Reprinted with permission from ref 27. Copyright 2016 Elsevier. (B) Customized FIA cell to perform electrochemical measurements on SPE under localized heat. Reprinted with permission from ref 28. Copyright 2008 Elsevier. (C) Miniaturized FIA instrumentation and 3D representation of the electrochemiluminescence resonance energy transfer reaction, where (a) Miniature peristaltic pump; b) Syringe; c) Spectroelectrochemistry instrument; d) Spectrometer; e) Bipotentiostat/galvanostat; f) Flow-cell connector; g) Reflexion probe; h) Flow-cell inline port; i) Flow-cell support holding electrode. Reprinted with permission from ref 29. Copyright 2017 Wiley-VCH. (D) Schematic representation of an FIA system for fenobucarb determination using GNRs-IL-CoPC/SPCE. Reprinted with permission from ref 30. Copyright 2019 Elsevier.

(intensity of peak current) in heated electrodes peak operating in a nonisothermal mode was attributed to the increase in mass and

charge transfer, as well as an increase in catalytic efficiency for ascorbic acid at elevated temperatures. The applicability of this

strategy was demonstrated by analyzing ascorbic acid in commercial orange juice samples.

Applications of SPCEs in ring-disc electrode configuration have also been demonstrated. By generating iodine in an FIA electrochemical cell with a wall jet configuration, As^{III} could be determined through a side reaction.³² Iodide (I^-) can be oxidized to iodine (I_2) at the disk electrode, and the electrogenerated I_2 was reduced back to I^- in the presence of As^{III} . The inhibited reduction current of I_2 to I^- was monitored at the ring electrode and related to the arsenic concentration in the sample. The proposed method was demonstrated for the quantification of As^{III} in groundwater (responsible for Blackfoot disease) in an endemic region close to Taiwan. Preanodized ring-disc SPCEs were used for direct (and simple) detection of monophenols (Figure 4A).²⁷ In this protocol, zinc phenol sulfonate (ZPS) was electro-oxidized on the disc electrode at $E_{\text{app}} = 1.5 \text{ V}$ vs Ag/AgCl, producing the quinone intermediates (1,2-dihydroxy, 1,4-dihydroxy, and 1,2,4-trihydroxybenzene) that were detected on a ring electrode at $E_{\text{app}} = 0.1 \text{ V}$ vs Ag/AgCl. The determination of ZPS as oxidized intermediates in cosmetics was demonstrated with satisfactory recovery values. This was the first electrochemical observation of monophenolic oxidation to redox active quinone species at a preanodized SPCE.

A thin-layer flow cell integrated with SPCE was used to develop electrochemiluminescence (ECL) based assays (Figure 4C) for monitoring hydrogen peroxide (H_2O_2). In this pioneering work, ECL transduction chemistry involving a donor-acceptor strategy between an electro-oxidized luminophore (luminol) and a fluorophore (fluorescein) was carried out.²⁹ The results showed an increase in the sensitivity for H_2O_2 detection compared to the classical luminol H_2O_2 -fluorescein assay.

A simple design of an electrochemical flow cell was presented by Hsu et al. using two foldable thick acetal platelets to enclose the SPE.³⁹ A cavity matching SPE dimensions was created in the bottom plate, and holes for the inlet and outlet were drilled in the upper plate. An O-ring was positioned over the electrode to promote sealing and to define the electrochemical area. The reference electrode was positioned in one of the sides, and a stainless-steel tube placed in the outlet was used as the counter electrode. The performance of the setup was evaluated using the well-known hexacyanoferrate system and applied to the quantification of glucose in human blood in an alkaline medium. The results obtained in this study were comparable with those obtained using a commercial YSI instrument.

A low cost, disposable microfluidic device ($\text{D}\mu\text{FD}$) containing an array of printed carbon electrodes was built to detect *Salmonella typhimurium* (*S. tryphi*). Tests for the detection of the bacteria were carried out in milk, using magneto-immunoassay, with labeled Au-NPs. Once *S. tryphi* is captured, it is separated from the sample using magnetic beads modified with monoclonal anti-*S. tryphi* antibodies followed by labeling with Au-NPs. The magneto-immuno-conjugate formed was injected into the $\text{D}\mu\text{FD}$ and magnetically attracted to the electrode surface by magnets positioned behind the unmodified array of electrodes. The approach presented a LOD of $7.7 \text{ cells mL}^{-1}$ and a linear range from 10 to 100 cells mL^{-1} .³¹ In a recent report, the electrochemical determination of three tumor biomarkers (homovanillic acid, vanillylmandelic acid and 5 hydroxyindole-3-acetic acid) was demonstrated with a LOD below $0.1 \mu\text{mol L}^{-1}$ for all analytes.⁴⁰

3.1.2. Screen Printed Electrodes Modified with Carbon Nanotubes (CNT). Due to the unique properties of carbon nanotubes (CNT) and their advantages in electrochemistry, SPEs modified with CNT have been widely explored. The analysis of paracetamol in pharmaceutical formulations was demonstrated achieving high analytical frequency (120 sample per hour) and low LOD ($1 \times 10^{-7} \text{ mol L}^{-1}$).⁴¹ Using a multiwalled SPE-CNT adapted in a homemade FIA cell, simultaneous determination of paracetamol and naproxen was reported.⁴² The use of multipulse amperometric detection increased selectivity and reduced interferences from the sample matrix.

A microflow system (requiring only $2 \mu\text{L}$ of sample) was developed and applied to the determination of estriol hormone in pharmaceutical samples, achieving an LOD of $0.53 \mu\text{mol L}^{-1}$ and analytical frequency of 32 samples per hour.⁴³ A simple method using a pretreated SPE modified with carbon nanofiber (CNF) was developed to analyze nimodipine (NMD) in pharmaceutical formulations and showed an RSD for precision and accuracy below 2%.⁴⁴ NMD concentration determined in drugs was in good agreement with those obtained using the pharmacopeia methodology. The determination of several nitro compounds (furazolidone, nitrofurazone, and nitrofurantoin) in chicken muscle was demonstrated using a commercial SPE-CNF and linear sweep voltammetry.⁴⁵ These works reveal the potential for using SPE-CNF-FIA as a new strategy for the rapid tracking of any drug derived from nitroaromatic compounds.

Searching for the enhancement of the sensitivity for H_2O_2 detection, homemade SPCEs were modified with CNT decorated with different metal NPs.⁴⁶ The best electrochemical response was obtained in palladium-CNT/SPCE, and it was explored for the quantification of H_2O_2 in disinfectant, hair colorant, and milk samples. A new method for the analysis of nitrofurantoin in urine samples without pretreatment was developed, and the comparison between SPE modified with CNF and CNT showed better reproducibility and sensitivity for the detection of these nitrofurantoin compounds in SPE-CNF.⁴⁷

An elegant approach was demonstrated by combining SPCE-CNT with an enzymatic column in an FIA system for the determination of hydroquinone.⁴⁸ Hydroquinone was oxidized to quinone in the column (by immobilized laccase) that was further detected amperometrically. The catalytic surfaces of modified SPEs were also evaluated as anodes in alcohol fuel cells. The activities of platinum NPs immobilized on carbon, CNT, and graphene nanoribbons toward methanol electro-oxidation were investigated. According to the authors, this method is robust, reproducible, and provides information that is closer to the real fuel cell scenario.⁴⁹

The determination of the insecticide fenobucarb was developed combining FIA and SPCE modified with graphene nanoribbons, ionic liquid, and cobalt phthalocyanine (CoPc) composites (Figure 4D). The amperometric current was obtained from the oxidation of 2-s-butyl-phenol, which is fenobucarb's product of alkaline hydrolysis. The proposed sensor yielded a sensitivity of $0.0884 \text{ mol L}^{-1} \text{ A}^{-1} \text{ cm}^{-2}$, a wide linear range from 0.025 to $110 \mu\text{mol L}^{-1}$, and a low LOD of $0.0089 \mu\text{mol L}^{-1}$. This was the first report applying nanocomposites for the modification of SPEs in order to quantify fenobucarb in vegetable samples.³⁰

3.1.3. Screen Printed Carbon Electrodes Modified by Metals. SPEs modified with metallic films have also been

explored, taking advantage of their unique catalytic properties or aiming to replace toxic metals with less hazardous ones. Lead at a trace level concentration could be measured with a gold-sputtered SPCE and voltammetric detection as an alternative to traditional mercury-based electrodes. This combination presented significant advantages in static cells, allowing a larger analyte preconcentration and minimizing environmental contamination.⁵⁰ A screen-printed gold electrode (SPAuE) and square wave voltammetry (SWV) were employed for the determination of nitromethane in air samples collected and delivered through the developed FIA system. According to the authors, nitromethane concentration in the air ranging from 8 to 90 ppm could be determined in 1–2 min.⁵¹ SPEs modified with gold nanoparticles have also been explored for the simultaneous determination of tryptophan and pyridoxine.⁵²

By using a screen-printed silver electrode (SPAgE) in an FIA system, aluminum chlorohydrate (ACH) was determined in antiperspirant samples by monitoring the free Cl^- ions liberated from ACH. The results obtained for four different real samples (with and without ACH content) were in good agreement with the product labels.⁵³ An SPCE modified with silver microcubes was employed for the determination of nitrite in meat, and the results were consistent with the spectrometric method.⁵⁴

SPCEs modified with copper have also been reported. Bromate content in hair waving products was determined using an electrode modified with nanocopper oxide.⁵⁵ An enhancement in the electrochemical reduction of bromate in acidic solutions was observed and attributed to the presence of Cu. Electrodes modified with Ni/Cu were also explored for glucose determination in several commercial beverages.⁵⁶ The arrangement of FIA-SPEs provided fast responses (120 samples/h), a large linear response ($1 \mu\text{mol L}^{-1}$ to 1mmol L^{-1}), and a low LOD ($0.33 \mu\text{mol L}^{-1}$). The sensor revealed good selectivity for glucose in the presence of interfering species (i.e., ascorbic acid, uric acid, acetaminophen, and other sugars).

A multisyringe flow injection analysis system (MSFIA) with a Bi film SPE was developed for the automated determination of cadmium (Cd) in natural waters. The high sensitivity of square-wave anodic stripping voltammetry (SWASV) combined with the designed MSFIA cell allowed the use of small volumes of reagents and sample, high sample throughput, and LODs below the limits established by European directrix. The cell was designed to allow easy replacement of the SPE, and its small size offered great portability.⁵⁷

3.1.4. Screen Printed Carbon Electrodes: Miscellaneous. Although bare SPCEs (or SPCEs modified with metallic films or CNT) are suitable to a wide range of applications, more elaborated modifications have been used to expand the analytical capabilities of these systems. The determination of isoniazid (INZ) in synthetic human urine samples was performed by using an SPCE modified with silver hexacyanoferrate.⁵⁸ The procedure proposed was employed for the direct determination of INZ in biological fluid samples and pharmaceutical formulations without the need for pretreatment of the sample. In another work,⁵⁹ INZ content in pharmaceutical formulations was determined by using an SPCE modified with CNF, chitosan (CHIT), and Au NPs. The Au^{3+} was drop casted onto CNF-CHIT film, followed by electrochemical potential cycling in order to generate the NPs.

A disposable SPCE modified with cobalt phthalocyanine (CoPc) was associated with FIA for the determination of zinc

pyrithione (ZPT) in hair care products, achieving an LOD of $0.9 \mu\text{mol L}^{-1}$ in 0.1mol L^{-1} KOH solution.⁶⁰ By using a commercial SPAuE modified with chitosan, sodium dodecyl sulfonate, and nickel(II) phthalocyanine tetrasulfonic acid, the voltammetric determination of 2-nitro-p-phenylenediamine in hair dyes was demonstrated.⁶¹ The response of this modified SPAuE for 2-nitro-p-phenylenediamine was also evaluated (in batch) using SWV and amperometry/FIA and led to LODs of 1.2 and $1.6 \mu\text{mol L}^{-1}$, respectively.

By modifying an SPE with carbon black NPs, the electroactive complex produced by the classical reaction between phosphate and molybdate could be reduced, and this allowed the continuous monitoring of phosphate in water.⁶² An SPE modified with Prussian Blue (PB) was used for the quantification of free chloride in tap and drinking water. In addition to the low LOD (8.25 ppb) obtained, no interference from other anions such as nitrate, nitrite, and sulfate was observed.⁶³

An SPCE modified with polyaniline/graphene quantum dots was used for the rapid determination of Cr(VI) employing stopped-flow coupled with linear-sweep voltammetry. An analytical frequency higher than 90 analyses per hour was attained, and the quantification of Cr(VI) in mineral water and in Cr-plating solutions was also demonstrated.⁶⁴

The construction of an integrated potentiostat for electrochemical sensing of urinary 3-hydroxyanthranilic acid under a flowing regime was described.⁶⁵ The measurements were performed in urine samples within the concentration range of 50–550 ng/mL, and a LOD of 3.1 pg/mL was obtained. Since the current range of this potentiostat is as low as a few nanoamperes, it has potential as a sensing array for a point of care system.

The development of SPEs based on stable pastes consisting of 2,2-diphenyl-1-picrylhydrazyl (DPPH) dissolved in ionic liquid was also described.⁶⁶ Its selectivity was demonstrated by analyzing catechol in the presence of potential interferents such as resorcinol and hydroquinone. The feasibility of the SPE was demonstrated for the detection of gallic acid in green tea by flow injection analysis.

3.2. Screen-Printed Electrodes Applied for Biosensing. While the development of biosensors using conventional electrodes started in the 1960s, the association of SPE biosensors with FIA only happened in 2003.⁶⁷ Nowadays, this association is attracting more attention, and this field is already well developed (as highlighted for the papers listed in Table 1), and single or arrays of SPEs containing immobilized enzymes can actually be bought commercially.²¹ At the current stage of this technology, researchers can acquire high quality commercial SPE sensors at a low cost, facilitating the reproducibility of the experiments by other researcher groups.

3.2.1. Glucose Sensors. Amperometric glucose biosensors have been prepared using different modifications in the SPE surface^{66–70} such as enzymes (glucose oxidase, glucose dehydrogenase, horseradish peroxidase) and metal oxides (like MnO_2 , CuO, and Fe_3O_4), among other molecules (graphene, Os-complex, and nanocomposites). The classical three electrode planar configuration was constructed using a screen-printing technique, where the biological recognition element was immobilized on the working electrode surface. In 2005, the first SPCE biosensor containing manganese oxide (MnO_2) as a mediator and the enzyme glucose oxidase (GOx) was described for applications in the FIA system for analysis of glucose in beer.⁶⁸

Another amperometric glucose biosensor containing GOx and Fe₃O₄ magnetic nanoparticles (NPs) decorated with gold was recently reported for food and drinks analysis. GOx was chemisorbed on these NPs and immobilized on a SPCE bulk-modified with MnO₂. The designed biosensor associated with a FIA system yielded a linear range from 0.2 to 9.0 mmol L⁻¹ with a sensitivity of 2.52 μA mmol⁻¹ L cm⁻² and a LOD of 0.1 mmol L⁻¹ for glucose. The synergic effect of MnO₂ as a mediator in combination with Fe₃O₄@Au resulted in an enhanced sensitivity, facilitating the enzyme immobilization and providing a wider linear range. The results obtained in glucose syrup samples, honeys, and energy drinks were in accordance with the glycosometer measurements.⁶⁹

A glucose biosensor based on the immobilization of the enzymes glucose oxidase and horseradish peroxidase was developed for measurement in an FIA system.⁷⁰ The enzymes were entrapped in the sol–gel matrices, and the Os complex (an excellent electron mediator) was immobilized by covalent linking for avoiding the leakage of the biosensor components. The reaction occurred throughout the three-dimensional network, without degradation of biomolecules, since the biosensor presented 90% of its original activity for about 14 months. Other characteristics of this sensor were a low working potential (−0.1 V vs. Ag/AgCl), linear responses in the 0.5 to 30 mmol L⁻¹ range, good reproducibility, fast response, and good sensitivity for FIA analysis.

An SPCE containing Meldola's Blue-Reinecke salt (MBRS) was designed to perform glucose measurements in serum. The electrode was covered with the enzyme glucose dehydrogenase and nicotinamide adenine dinucleotide coenzyme (NAD⁺).⁷¹ The amperometric flow system operated at a +0.05 V vs Ag/AgCl working potential. This study demonstrated the association of MBRS-based sensors with FIA, producing electrocatalytic oxidation in the presence of NADH.

A nonenzymatic biosensor, constituted of a CuO/graphene nanocomposite applied on an SPE, was explored for quantification of glucose integrated with a FIA system in 0.1 mol L⁻¹ NaOH as an electrolytic solution.⁷² The observed low LOD (34.3 nmol L⁻¹) and the high sensitivity (of 2367 μA mmol⁻¹ L cm⁻²) are attributed to the advantages of FIA (like the elevated mass transport) as well as a rough SCPE surface. Negligible interference was demonstrated for ascorbic acid, uric acid, dopamine, fructose, lactose, and sucrose.

3.2.2. Pesticide's Detection. Cholinesterase is the family of enzymes applied in the SPE modification for pesticide detection, especially in water samples. The first SPE biosensor for the screening of organophosphorus pesticides in a FIA system was prepared by entrapping the enzyme anticholinesterase (AChE) in an Al₂O₃ sol–gel matrix screen-printed on an integrated three-electrode chip.⁷³ This strategy increased the stability of the enzyme AChE but also catalyzed the oxidative reaction of thiocholine. The intense electrocatalysis provided by the biosensor made up of Al₂O₃–AChE allowed the substrate to be detected in seawater and distilled water, hundreds of mini-volts below the potentials reported in other articles.

The detection of organophosphate insecticides (OIs) using acetylcholinesterase was also demonstrated in a flow based electrochemical system. Here, magnetic beads were used as support for immobilized AChE, allowing the automatic regeneration of SPE surface. In this work, a renewable magnetic NPs based sensing was designed and integrated in

an automatic flow platform for the online monitoring of OIs in water samples.⁷⁴

A butyrylcholinesterase based biosensor inserted in a flow system for the detection of the organophosphorous pesticide paraoxon was built by immobilization on a SPE modified with Prussian Blue (PB) NPs. The quantification of the enzymatic hydrolysis was performed before and after the exposure of the biosensor to paraoxon, and measurement of the thiocholine product. This biosensor evaluated the paraoxon inhibitory effect at the parts per billion level, and it was also tested in drinking, river, and lake water samples. The advantage of this system is the determination of cholinesterase enzyme inhibitors (organophosphorus and carbamate pesticides) in samples without pretreatments and to automate the analyses, reducing costs and time.⁷⁵

Du and co-workers⁷⁶ developed an SPE-CNT integrated with a microflow arrangement for biosensing (via reactivation of cholinesterase) of organophosphorus (paraoxon) for in vitro inhibition in rat saliva. Two other biosensors were built using AChE and employed to detect chlorpyrifos-oxon and malaoxon in milk samples.⁷⁷ The simultaneous determination of the binary organophosphates was demonstrated for six milk samples using the automated flow-based biosensor.

3.2.3. Phenolic Compounds. The determination of phenolic compounds has been reported using different modifications in the SPE surface^{66–70} such as enzymes (laccase, tyrosinase, and horseradish peroxidase) and gold nanoparticles (AuNPs), among other molecules (graphene and carbon-nanotubes). SPCE immobilized with horseradish peroxidase gave nanomolar LODs for catechol (110.2 nmol L⁻¹), dopamine (640.2 nmol L⁻¹), octopamine (3341 nmol L⁻¹), pyrogallol (50.1 nmol L⁻¹), and 3,4-dihydroxy-L-phenylalanine (980.7 nmol L⁻¹) determination.⁷⁸ A laccase SPE biosensor containing AuNPs and fullerenols was assembled using the layer-by-layer procedure.⁷⁹ This biosensor was tested toward gallic acid (usually explored as a standard for polyphenols analysis of wines), showing good stability and sensitivity joined with FIA/amperometry.

SPCEs were modified with CNT and AuNPs followed by covalent binding with tyrosinase and combined with a microfluidic device based on commercial textile threads for phenol detection. The FIA-SPCE biosensor proposed exhibited recovery values in tap water within the range of 89–100%.⁸⁰ Another tyrosinase biosensor was assembled on a commercial SPCE covered by a graphene cross-linked with glutaraldehyde and a layer of nafion. The biosensor was successfully applied for FIA-amperometric determination of acetaminophen in human urine from healthy volunteers at 0.0 V vs a silver reference electrode.⁸¹

3.2.4. Other Applications. The first study associating SPE, FIA, and biosensing was developed for the detection of NADH (dihyronicotinamide adenine dinucleotide) in phosphate buffer.⁸² NADH is a very important cofactor, and its quantification can be related to enzymatic reactions. The modification of the SPCE by the electro-oxidative polymerization of thionine made its surface free of poisoning, favoring reproducible signals with good stability.⁸² In the following year, the same research group described an alternative approach for the determination of NADH using the FIA system associated with SPCE.⁸³ A new polymeric film was prepared on the electrode surface by the oxidative electro-polymerization of azure A or toluidine blue O in PBS. The resulting modified SPCE exhibited good electrocatalytic

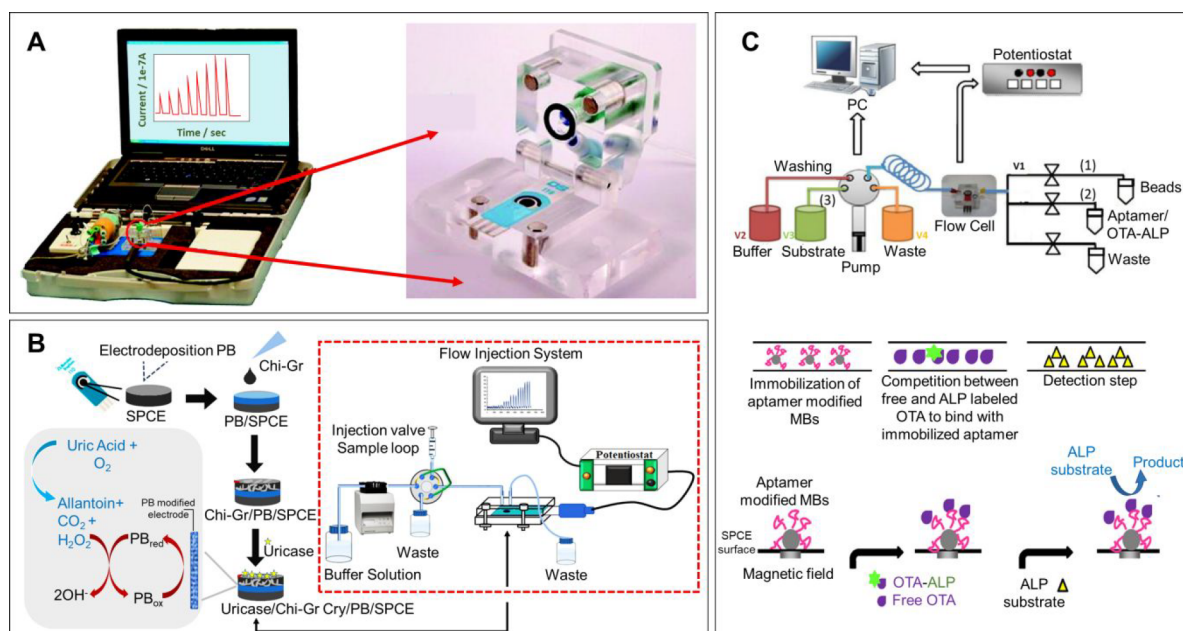


Figure 5. Examples of SPE-FIA biosensors applications. (A) The entire analytical system, emphasizing the sensing area. Reprinted with permission from refs 76 and 81. Copyright 2009 Elsevier. (B) Preparation process of uric acid enzyme biosensor based on an SPE coated with Prussian Blue and modified with chitosan-graphene composite cryogel. The modified SPE was used in an FIA-amperometric system. Reprinted with permission from ref 90. Copyright 2020 Elsevier. (C) Flow injection system used in the automation of ochratoxin A (OTA) aptasensor, evidencing the direct competitive format. Reprinted with permission from ref 87. Copyright 2013 Elsevier.

activity and stability for NADH oxidation, with LOD estimated to be $2 \times 10^{-7} \text{ mol L}^{-1}$ and a linear range of $0.5\text{--}100 \mu\text{mol L}^{-1}$.

Examples of studies performed for SPE biosensors in association with FIA are listed in Figure 5. An SPCE containing Meldola's Blue-Reinecke salt (MBRS) covered with the enzyme lactate dehydrogenase and NAD^+ was developed to measure lactate in serum.⁸⁴ The entire analysis system, emphasizing the sensing area, is represented in Figure 5A. The biosensor was incorporated into a commercial amperometric flow system operating at $+0.05 \text{ V}$ working potential vs Ag/AgCl . This same strategy can be applied to other dehydrogenase enzymes, which may produce amperometric biosensors for other clinically important compounds.

A flow injection immunoassay based SPCE was developed for the enzyme immunoassay of antigen.⁸⁵ The flow immunoassay was performed at 0.0 V (vs Ag/AgCl) within the linear range of $30\text{--}700 \text{ ng mL}^{-1}$ and a LOD of 3 ng mL^{-1} (both situated in the nanograms region). The use of a flow amperometric cell with an integrated magnet was also reported for biotin determination, exploring magnetic bead assays.⁸⁶ The reaction is based on a competitive assay between free biotin and biotin with horseradish peroxidase. The linear range and sensitivity obtained were also situated in the nanomolar region (from 0.01 to 1 nmol L^{-1} and $758 \text{ nA nmol}^{-1} \text{ L}$ respectively). The modification and cleaning of the electrode were performed by removing the magnet from the electrode region. This procedure turned the cleanup of the electrode very rapid, and more analysis could be obtained in a short time.

A flow-based aptasensor with magnetic beads was employed for the detection of ochratoxin A (a toxic metabolite, produced by several fungal species, present in many foods).⁸⁷ In the direct strategy, biotin and free ochratoxin A competed to bind with the immobilized aptamer onto the SPCE surface in a flow cell (Figure 5C). In the indirect assay, immobilized and free

ochratoxin A in solution competed to bind with aptamer in solution. The lowest LOD (50 ng L^{-1}) was observed in the indirect flow-based aptasensor for real beer samples.

Iridium oxide NPs and tyrosinase were immobilized onto SPE, and this system was evaluated in batch (via chelating copper at the active site of tyrosinase) and in flow mode (by thioquinone formation). Both systems are very sensitive with a nanomolar LOD, added to the advantages of the flow system, being its reusability, automation, low sample volume ($6 \mu\text{L}$), and fast response (20 s).⁸⁸ The quantification of low volumes of methimazole was described using an amperometric lab on a chip microsystem and applied to spiked human serum and pharmaceutical dosages.

Screen-printed graphitic electrodes (SPGEs) modified with Prussian Blue (PB) and uricase were proposed for the electrochemical detection of uric acid (UA) in urine samples. Uricase was immobilized through physical adsorption, and the modified SPGE was coupled to a flow cell (Figure 5B). The biosensor responded linearly to UA in the range of 10 to $200 \mu\text{mol L}^{-1}$, with a LOD of 3.0 mmol L^{-1} .⁸⁹ Another SPCE biosensor was developed by immobilizing uricase on graphene-incorporated chitosan (Chi) on the top of a PB layer electrodeposited electrode.⁹⁰ The detection of UA was favored by the presence of PB and combined with flow system, with a detection potential of 0.0 V . The biosensor showed a large linear range (0.0025 and 0.40 mmol L^{-1}) with a micromolar LOD, providing great stability that enabled reuse up to 175 times ($\text{RSD} = 3.7\%$). The modified SPCE presented no response from the common interfering species present in human serum, and the developed UA biosensor was associated with FIA achieving recoveries ranging from $(98 \pm 2)\%$ to $(102 \pm 5)\%$ in blood samples.

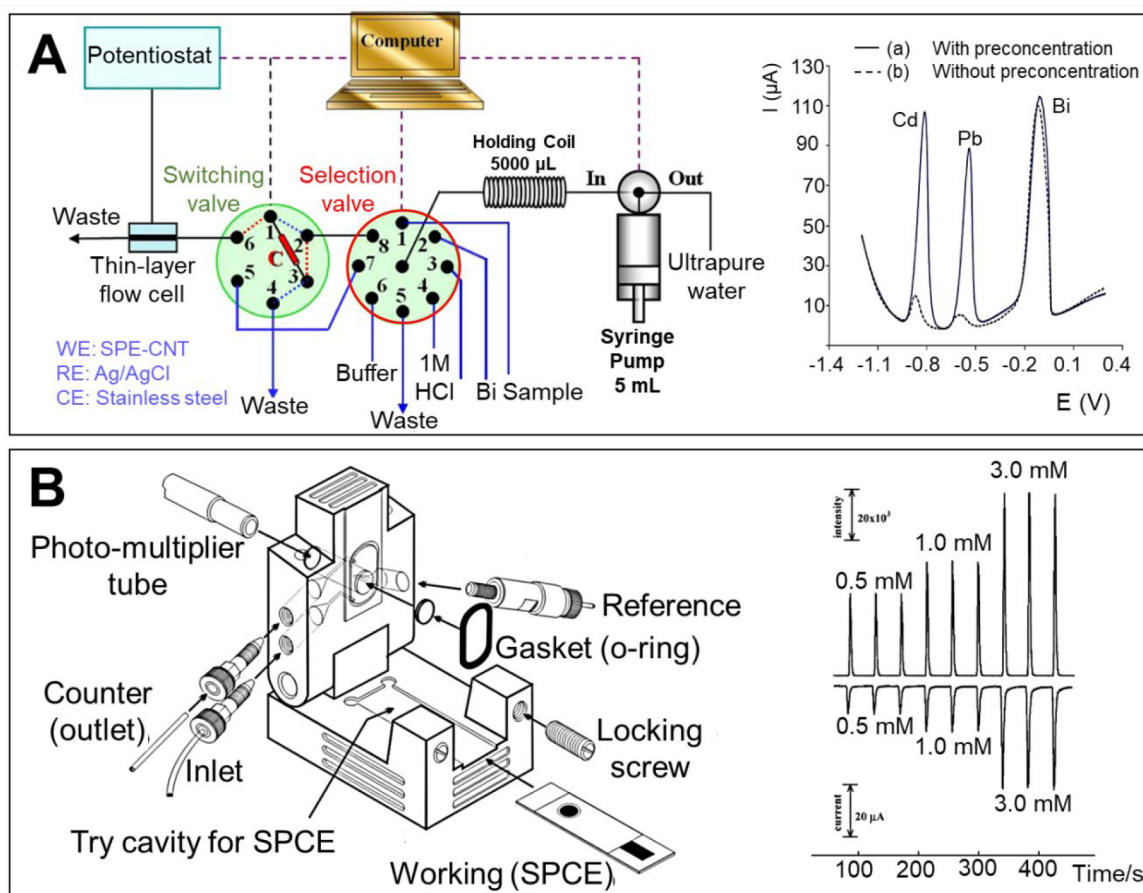


Figure 6. Examples of SPE-SIA applications. (A) SIA-ASV system for preconcentration and determination of Pb(II) and Cd(II). Comparison of the voltammograms from the square-wave ASV of a solution containing Pb(II) and Cd(II) ions in an acetate buffer. Reprinted with permission from ref 93. Copyright 2005 Elsevier. (B) Device specifically designed for a disposable SPCE. Electrochemiluminescence and amperometric signals for triplicate injections of oxalate + 100 μM Ru(bpy) $_3^{2+}$ at a bare SPCE. Reprinted with permission from ref 96. Copyright 2007 Elsevier.

4. SEQUENTIAL INJECTION ANALYSIS (SIA)

Sequential injection analysis (SIA) and batch injection analysis (BIA) are automated techniques developed to fill some gaps existent in the flow-injection methodology. SIA consists of multiple valves and a syringe pump, exhibiting potential for coupling with anodic stripping voltammetry (ASV) due to its simplicity and convenience for sample manipulations.¹⁰ Various stripping voltammetric methods associated with the SIA system have been reported for heavy metal analyses.⁹¹ ASV has been used for the determination of trace heavy metal ions due to its sensitivity from both the preconcentration step and the measurement procedure.⁹² Furthermore, combining ASV with a flow system (Figure 6A) has advantages including an improvement in accuracy, speed of analysis, and precision; potential for automation; reduction of risk contamination; and cost-efficiency, among others.⁹³

The process of ASV for the determination of heavy metals involves the electrochemical deposition or accumulation of the target metal onto a suitable electrode at a more negative potential than the standard potential of this metal for a few minutes. After this deposition, the accumulated metals on the electrode surface are oxidized using a reverse potential scan. Many researchers have reported use of the Bi film electrode because it is inexpensive, disposable, and easy to produce.¹⁹ The Bi working electrode can be constructed by electro-deposition on the substrate (SPE) in an effort to improve the

sensitivity of heavy metals.²⁰ Most of the SPEs approached in this section were based on electrodes modified with Bi films, as listed in Table 2. Bismuth surfaces are very favorable for deposition of metals, and this condition is very suitable for their determination at trace levels.

A Bi film was prepared on the SPE-CNT, and the practical utility of the method was also demonstrated with the simultaneous determination of Pb(II), Cd(II), and Zn(II) at low microgram per liter concentration levels via an SIA-ASV procedure in herb samples.⁹⁴ In another study, the Bi film was deposited simultaneously with the analyte on the modified electrode, resulting in a highly sensitive Bi film modified SPCE. The results demonstrated that coupling Bi-SPCE with SIA-SWASV provides an environmentally friendly tool to perform rapid, low cost, and automated determination of Pb $^{2+}$ and Cd $^{2+}$ in rice samples.⁹⁵

In 2007, the first flow cell was designed to simultaneously perform amperometry and electrochemiluminescence (ECL) associated with SIA on an SPCE (Figure 6B). The amperometric signals were obtained in the conventional way, while the luminescence signals were collected via an optical fiber positioned exactly in front of the electrode and transferred to the photomultiplier. A major advantage of the proposed cell is the considerable reduction of the sample and especially of the chemiluminescence inductor (Ru(bipy) $_3^{2+}$ salt). The combined ECL and amperometric signals were used to detect oxalate in nanomolar to millimolar ranges.⁹⁶

Table 2. Studies Involving Screen-Printed Electrodes (SPE) Associated with SIA and BIA^a

electrode material	analyte	sample (matrix)	detection method	linear range ($\mu\text{mol/L}$)	LOD ($\mu\text{mol/L}$)	detection potential (V)	flow rate ($\mu\text{L/min}$)	ref
Bi-SPE-CNT	Pb(II), Cd(II), and Zn(II)	herbs	SWASV*	2–100, 2–100, and 12–100	0.2, 0.8, and 11	–1.4 to 0.1	12	94
Bi-SPCE	Pb ²⁺ and Cd ²⁺	rice	SWASV*	0.5–60	0.11 and 0.27	–1.0 to –0.3	12	95
SPCE	oxalate	aqueous solution	amperometry	10–5000		1.2	300	96
Au-SPCE	As(III)	water	differential pulse – ASV	1–100	0.03	–0.1 to 0.5	600	97
SPAuE	As(III)	water	SWASV*	0.1–1.0	0.02	–0.4 to 0.4	900	98
SPAuE	Hg(II)	complexation by humic acid	SWASV*	0.050 and 0.50	0.017	0.3 to 0.7	900	99
Au-SPCE	Hg(II)	water	SWASV*	1–20	0.22	–0.5 to 0.2	600	100
graphite-SPE modified with Hg	Cu(II), Pb(II), Cd(II) and Zn(II)	water	SWASV*	2.5–500	1.3, 1.4, 0.6, and 4.2	–1.4 to –0.3	600	101
Sb film-graphene oxide-SPCE	Cd(II), Pb(II), Cu(II), and Hg(II)	water	SWASV*	0.1–1.5	0.05, 0.03, 0.06, and 0.07	–1.0 to 0.4	600	102
SPCE-CNT	paraquat	water	DPV*	0.54–4.30	0.17	–0.3 to –0.9	6000	103
graphene oxide-SPCE	immunoglobulin G	urine	amperometry	2–100 ng mL ⁻¹	1.70 ng mL ⁻¹	0.35	2000	104
SCPE-graphene	diclofenac	pharmaceuticals	amperometry	30 – 3 × 10 ⁻³		0.8	53	108
Prussian Blue - SPE	H ₂ O ₂	blood serum	amperometry	up to 1000	0.12	0.0		108
SPGE	Pb, Cu, and Hg	biodiesel	SWV		0.02, 0.03, and 0.02	0.55	16.4	108
SPCE	H ₂ O ₂ and paracetamol	artificial buffer	amperometry	25–175		0.0 and 0.1	32 and 60	113
SPCE	catechin	plant extracts	amperometry	1–150	0.021	0.3	77	114
SPE-CNT	carbendazim, catechol, and hydroquinone	tap water	amperometry	0.2–100, 0.1–200, 0.1–200	0.06, 0.05, 0.02	0.8, 0.5, and 0.3	155	115
SPGE	2,6-ditert-butylphenol	liquid fuels	amperometry	2.5–25 ($\mu\text{g/L}$)	290 ($\mu\text{g/L}$)	1.1	53	116
SPAuE	lead	aviation fuel	SWASV*	10–750 ($\mu\text{g/L}$)	0.0008 and 0.071 ($\mu\text{g/L}$)	–0.45 to –0.05	4.8	117
SPGE	2,5-dimercapto-1,3,5-thiadiazole	fuel ethanol, seawater and mineral oil	amperometry	5–75	0.3	1.1	193	118
polyester-SPGE	2,2-diphenyl-1-picrylhydrazyl	food	amperometry	1–10 ($\mu\text{g/L}$)	1	0.1	193	119
graphite organic-resistant SPE	levamisole and sodium levothyroxine	aqueous and hydroethanolic media	amperometry	1–100	0.1	0.8	25	120
SPAuE	Pb, Cu, and Hg	biodiesel	SWASV*	20–280 ($\mu\text{g/L}$)	1.0, 0.5, and 0.7 ($\mu\text{g/L}$)	–0.4 to 0.6	5	121
SPE-CNT	omeprazole	pharmaceutical	amperometry	1–50	0.09	1.1	32	122
SPE-CNT	ciprofloxacin	pharmaceutical	amperometry	5–75	<0.1	1.0	153	123
SPCE	benzocaine and tricaine	fish fillets	amperometry	0.1–8.0	0.03	0.9 and 0.75	271	124
SPAuE	Cd, Pb, Cu, Zn, and Hg	biodiesel	SWASV*	up to 450 ($\mu\text{g/L}$)	4.5, 2.2, 6.7, 7.5, and 4.0 ($\mu\text{g/L}$)	0.25 to 0.6	53	125
AuNPs -GOx -SPCE	glucose	artificial serum	amperometry	1000–10 000	110	–0.25	28	126
SPE-CNT	uric acid and nitrite	urine, saliva, and blood	amperometry	1–500	0.05 and 0.06	0.45 and 0.7	277	127
SPCE	tert-butylhydroquinone	perchloric acid	amperometry	1–1000	0.18	0.5 153		128

^aASV, anodic stripping voltammetry; CNT, carbon nanotube; DPV, differential potential voltammetry; LOD, limit of detection; SPAuE, screen-printed gold electrode; SPCE, screen-printed carbon electrode; SPE, screen-printed electrode; SPGE, screen-printed graphitic electrodes; SWASV, square-wave anodic stripping voltammetry.

SIA has been performed mostly for the detection of metals in water samples. An automated method based on SIA-ASV with a gold deposited on an SPCE was developed for inorganic arsenic determination.⁹⁷ The large amount of Au on the SPCE headed to an increase in roughness and surface area, which allowed a low LOD for As(III) ($0.03 \mu\text{g L}^{-1}$). This study was the first to report a long durability of Au-modified SPCE, since it was used for three working days, carrying out more than 300 analyses and maintaining a low standard deviation.

SIA has been also associated with SWV, especially using SPAuE for the determination of metals. Arsenic has great affinity for gold surfaces, and the use of SPAuE avoids the need to prepare Au films, which involves the consumption of Au(III) solutions. The limit of As(III) quantification obtained using this system was almost 2 times lower than the maximum concentration of As(III) allowed in river waters ($10 \mu\text{g L}^{-1}$).⁹⁸ The quantification of mercury(II) by SIA-SWV was also demonstrated using SPAuE through humic acid complex-

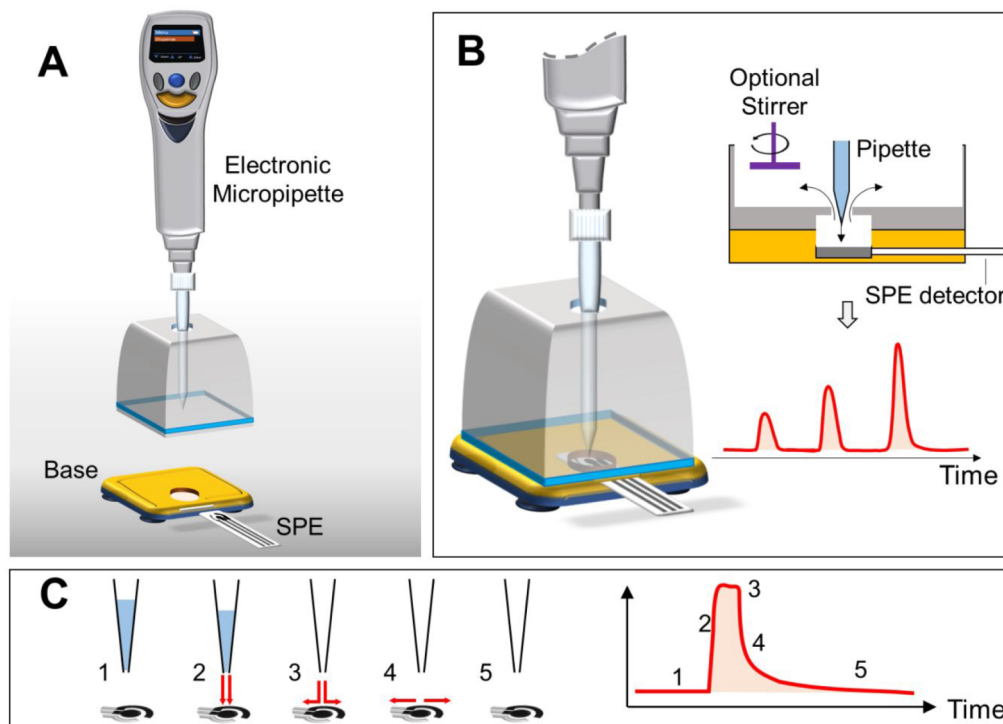


Figure 7. Schematic illustration of a BIA system. (A) BIA electrochemical system containing the micropipette on the top, the cell in the middle, and the electrode in the bottom. (B) Assembled cell and cross section showing the sample delivery and corresponding signal recorded. (C) Schematic showing the mass transport on the electrode surface upon a sample injection and respective signal. (Step 1) before the injection, (step 2) transport during the injection, (step 3) end of the injection, (step 4) washing out, (step 5) final equilibrium.

ation.⁹⁹ In this study, the speciation of Hg(II) in humic acid by stripping voltammetry was developed. A similar work for the determination of mercury(II) concentrations was developed using SIA-SWASV and in situ gold-film SPCE.¹⁰⁰ This system was used for the determination of Hg²⁺ concentration in drinking water and in chloride-rich samples. Applications for samples with 75% (v/v) seawater ($\sim 46 \text{ g L}^{-1}$ salinity) and 200 g L^{-1} salt were done with good accuracy.

Studies involving the quantification of metal ions such as Cu^{II}, Pb^{II}, Cd^{II}, and Zn^{II} in waters and sediments by SIA-SWASV were also described using SPGEs modified by electrodeposition of mercury.¹⁰¹ The proposed sensor modified with Hg⁰ was adequate for environmental analyses. The accuracy of the method resulted in recovery rates near 100% of the spiked concentrations, and for all four metals the limits are below of the values defined by regulatory agencies.

Simultaneous determination of heavy metals in water samples by SIA-ASV was reported using antimony-graphene oxide modified SPCE.¹⁰² The proposed chemically modified electrode was synthesized via reduction of antimony film by in situ electrodeposition and exhibited linear range from 0.1 to 1.5 mmol L^{-1} . Applications of this electrode for Cd(II), Pb(II), Cu(II), and Hg(II) quantification in water samples led to responses with an accuracy between 94 and 113% recovery.

The combination of SIA with differential pulse voltammetry (DPV) techniques using SPE was also found in the literature, aiming to provide high sample throughput, fast analysis, and low reagent consumption.¹⁰³ SPCE modified with CNT dispersed in Nafion and ethanol gave the best result for trace analysis of an herbicide (paraquat) using SIA-DPV. The proposed system showed no good response to interference

ions in contaminated natural water, surfactant, and other pesticides, without pretreatment of the samples.

Amperometric immunosensors were also developed by employing SPCE modified with graphene oxide (GO) and covalently attaching antihuman immunoglobulin G (anti-HIgG) for sensitive determination of HIgG. The SIA system was used to determine HIgG by immobilizing anti-HIgG on a GO modified SPCE.¹⁰⁴ The selective immunointeraction of HIgG to anti-HIgG was followed through the measurement of $[\text{Fe}(\text{CN})_6]^{3-/4-}$ redox current in PBS solution. The decrease of current recorded was proportional to HIgG concentration, revealing a linear response in the range of 2 to 100 ng mL^{-1} HIgG for urine samples.

5. BATCH INJECTION ANALYSIS (BIA)

BIA was proposed around 30 years ago by Wang and Taha, as a new system to perform rapid analysis.¹² In comparison to FIA, BIA is simpler, requiring only an injector, which is usually an electronic micropipette ($20\text{--}200 \mu\text{L}$) that replaces peristaltic pumps, tubing, and valves, ensuring the reproducible flow rate and injection volume. It is considered a tubeless FIA system¹⁰⁵ presenting similar advantages (sampling rate, sample size, accuracy, sensitivity, and reproducibility). Extra advantages come from the absence of additional components commonly required by FIA systems avoiding possible problems such as leaks or air bubbles. Furthermore, the batch configuration of the BIA electrochemical cell can be less destructive to SPE, overcoming unstable behavior due to the continuous flow of the carrier electrolyte.¹⁰⁶ However, FIA systems still can provide online reactions prior to detection (sample reaction, complex formation, extraction, precipitation, etc.) that are not so simple to implement in BIA systems.¹⁰⁷

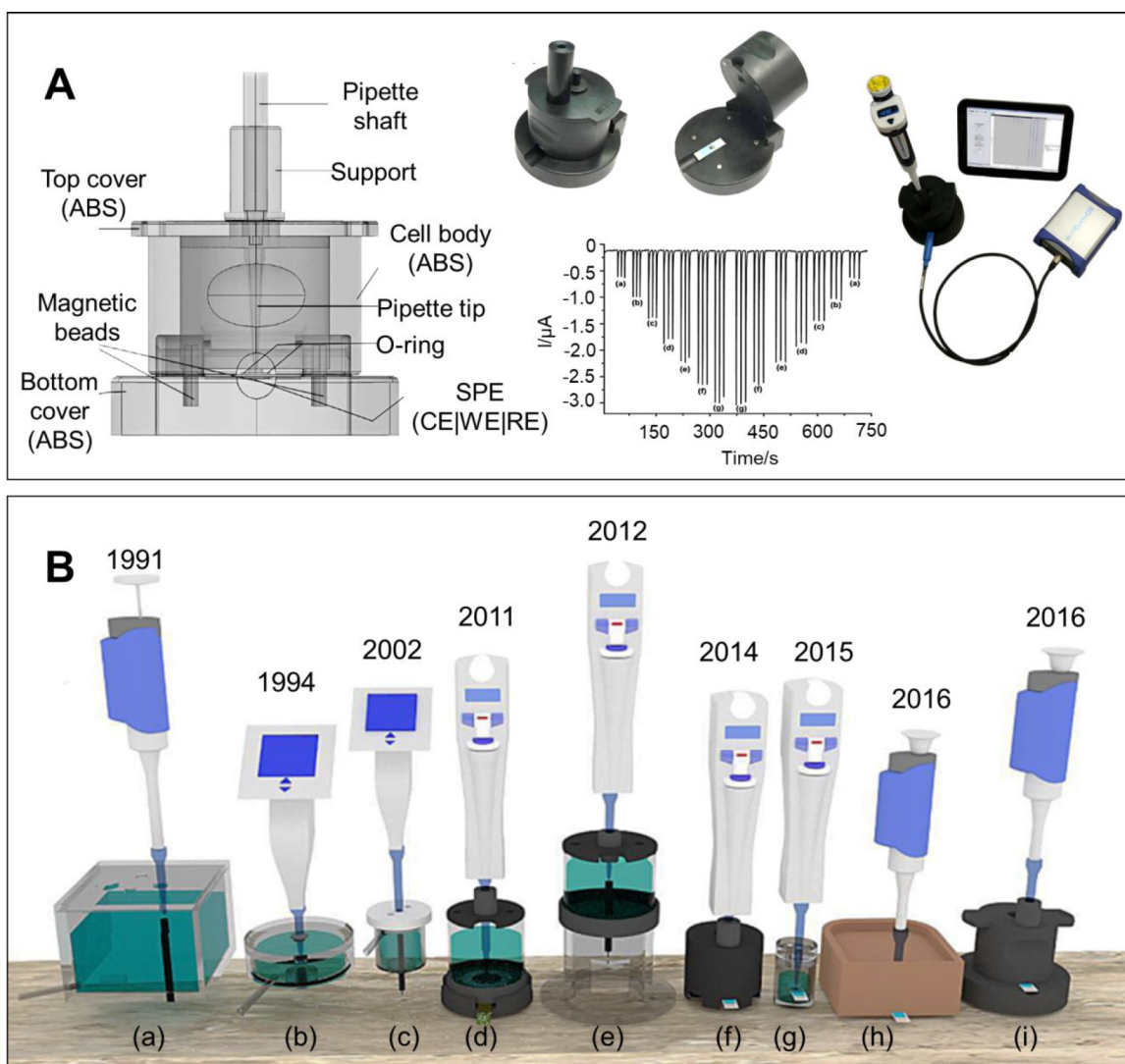


Figure 8. (A) Detailed design of a commercial batch injection analysis cell for screen printed electrodes. ABS: Acrylonitrile Butadiene Styrene. BIA results for amperometric detection of H_2O_2 with a carbon SPE modified with Prussian Blue. Reprinted with permission from ref 113. Copyright 2016 Elsevier. (B) Chronology of different BIA systems developed by different research groups. Reprinted with permission from ref 15. Copyright 2018 Elsevier.

Additional advantages of BIA systems are easy transport, the use of its components with low power consumption, and its commercial availability. These characteristics make BIA most suitable for in field use, requiring only battery-powered accessories such as an electronic micropipette and a potentiostat connected to a laptop or tablet (or even to a cell phone via bluetooth). Therefore, the set consisting of the BIA cell and SPE has great potential to be operated outside a laboratory, in the absence of an external power supply as a robust convenient electroanalytical system.¹⁰⁸

The BIA system is based on the injection of a sample through a micropipette tip directly in the working electrode surface immersed in an electrolytic solution (Figure 7). The coupling of BIA with electrochemical detectors provides advantages for applications in the analytical chemistry field, offering adjustable selectivity, high sensitivity, high sampling rates, accuracy, and precision. Among the electrochemical methods, amperometric detection has been the most popular technique used in BIA systems.¹⁵

The first BIA cell was large, in order to contain enough volume of electrolyte to ensure a huge factor of dilution for the

injected solution. Over time, we learned the fantastic difference between the transport speed to the electrode during the injection of the analyte and its diffusional transport after ceasing the movement of the solution. The injections correspond to the transport of electroactive material to the electrode surface at a high centimeter per second rate, whereas the diffusion of the analyte generally is on the order of $10^{-6} \text{ cm s}^{-1}$.¹⁰⁹ However, in our recent studies, cells with a volume of only 4 mL were successfully used.¹¹⁰

After the tank is filled with the electrolyte, the BIA cell is closed with a lid containing four holes, one positioned on the electronic micropipette, two others to introduce the reference and counter electrodes, and the last to introduce a stirrer interface (when necessary). The position of the micropipette tip is centered on the top of the electrode surface, and the distance between the tip and the electrode surface remains constant. These two parameters contribute significantly to the reproducibility of the procedure.¹⁵

Until 2014, SPE and BIA systems were separately used in the development of methods with portable characteristics.¹⁰⁸ However, the growing popularity of 3-D printers allowed

scientists to build their own cells, improving the association of SPE and BIA.¹¹¹ The BIA system for SPEs yielded similar results to those obtained by FIA, but without the need of additional components, such as tubes, pumping, and injection valves. This cell was improved and in the following years was converted in a commercial product.¹¹²

Specific details on the fabrication and operation (cell assembly, positioning of the SPE in the cell, electronic micropipette operation, etc.) can be accessed in videos available on the Internet.¹¹² The proposed system has several characteristics required for portable instruments: (i) short time analysis, (ii) easy operation, (iii) low acquisition and operation cost, (iv) low energy use, (v) reduced reagent use, (vi) minimal sample pretreatment, (vii) safety for the operator, and (viii) minimal waste generation. Considering the characteristics of BIA cells and SPEs individually, the system that combines both has great potential to be used as a portable electrochemical tool in laboratories with minimal infrastructure.¹¹¹

The commercial BIA cell¹¹³ was first published in 2016 and consists of a cylindrical cup, to which a foldable base at the bottom has been adapted (Figure 8A). At the base of the cell, there is a hole with the exact dimension of the SPE electrode, and on the outside, there is a groove to fit an O ring, preventing the leakage of solution. The proposed portable system shows several advantages that include small volumes of samples, excellent cost effectiveness, and ease of operation (“user-friendly”). BIA cells have usually been fabricated in glass or polymeric materials like Plexiglas and polypropylene, and a chronology of different BIA cell designs developed over the years is presented at Figure 8B.

Most BIA studies developed in this section utilized SPCE for determinations in pharmaceuticals, food samples, and plant extracts, among others.^{108,113,114} SPE-CNT was also mostly chosen for determinations in tap water, pharmaceutical, urine, saliva, and blood samples, presenting better stability associated with BIA when compared to conventional FIA cells.¹¹⁵ Another recurring application is the analysis of metals and antioxidants in different fuel samples (biodiesel, ethanol, and aviation fuels) as highlighted in Table 2.^{116–118}

An organic-resistant SPGE was built by using insulator inks on a polyester substrate, producing an arrangement highly compatible with liquid fuels. Applications for monitoring antioxidants in aviation jet fuel and in biodiesel revealed comparable results for BIA with liquid and gas chromatographic analyses.¹¹⁶ A similar study provided great promises for lead trace quantification in aviation (bio)fuel samples using SPAuE associated with anodic stripping voltammetry.¹¹⁷ The continuous monitoring of a corrosion inhibitor was also demonstrated for ethanol, seawater, and mineral oil with rapid (180 analysis h⁻¹) and precise (RSD < 3%) response, with a low LOD (0.3 μmol L⁻¹) related to the analyses.¹¹⁸

Amperometry has been utilized as the main detection method associated with BIA-SPE.^{113–116,118–120} The remaining 25% of the works found within this section focused on the association of square wave voltammetry with BIA,^{117,121} especially involving anodic stripping. In terms of samples evaluated, pharmaceuticals such as paracetamol, diclofenac, omeprazole, and ciprofloxacin have been the most determined using the configuration BIA-SPE.^{108,113,120,122,123}

A graphite organic-resistant SPE was assembled in a BIA cell to perform the determination of pharmaceutical molecules (levamisole and sodium levothyroxine). The analyte adsorp-

tion on the electrode surface was solved using a fast electrode cleaning supplier adapted to the cell by external stirring, which extended the lifetime of such a sensor. The proposed method showed great potentiality for the determination of a wide range of pharmaceuticals, providing faster analysis than previous works published in the literature for FIA and HPLC.¹²⁰

A multiwalled SPE-CNT coupled to the BIA was employed for the amperometric determination of omeprazole in pharmaceutical samples.¹²² The results obtained through this system allowed the attainment of a nanomolar LOD (9 nmol L⁻¹) and provided superior performance to that of FIA, with microliter sample volumes injected by an electronic micropipette. The use of SPE simplified the analysis, once the three electrodes came together in a single support, making the system easily adapted for portable analyses. The BIA system provided superior sensitive detection to that of FIA due to the higher flow rates of the solutions injected at the electrode surface.¹²³

A system based on BIA-SPCE with amperometric detection was applied for the quantification of anesthetics compounds (benzocaine and tricaine) in fish tissues.¹²⁴ The proposed method allows the performance of rapid analysis (over 300 injections per hour) with a low LOD (3.02 × 10⁻⁸ mol L⁻¹ for benzocaine and 3.19 × 10⁻⁸ mol L⁻¹ for tricaine). The simple sample preparation reduced significantly the amount of fat in the fish extract, favoring precision (recovery values above 99% for both analytes).

SPAuE has been successfully associated with ASV for the determination of trace metals in biodiesel and aviation fuel.^{117,121} This voltammetric detection presented the advantages of low sample consumption, which extended the SPAuE lifetime to a whole working day of analyses, due to the consequent reduction of electrode fouling.¹²¹ The disposable SPAuE can be adapted to a BIA cell, presenting lower sensitivity than conventional systems that can be associated with on-site electroanalysis.¹²⁵

The association of BIA and SPCE biosensors has been reported as well to promote the enzymatic analysis of glucose in artificial serum. Gold nanoparticles (AuNPs) and glucose oxidase were covalently immobilized on the top of the electrode for the electrochemical detection. The development of paper-based enzymatic reactors was described using a 3D printed BIA cell, and the cell was used for more than one year without maintenance or damage.¹²⁶ The reaction product of the enzymatic reaction (H₂O₂) was collected with an electronic micropipette in a microtube and analyzed in the 3D BIA cell coupled with the SPE modified with Prussian Blue. The use of a 3D printer allowed the fabrication of a BIA cell in a relatively short processing time (within 4 h, in a one-step manufacturing) at a cost of about \$5.

Simultaneous determination using BIA-SPE associated with multiple-pulse amperometry (MPA) detection was performed for urine, saliva, and blood samples to detect UA and nitrite. As a comparison, a differential-pulse voltammetric (DPV) method was performed, using the SPEs modified with multiwalled CNT. BIA-MPA was more highly precise (RSD around 1%), faster (160 h⁻¹), and free from sample interference as recovery values ranged from 77 to 121%. On the other hand, recovery tests conducted using DPV did not provide adequate recovery values (>150%), probably due to the longer contact time of the SPE with the biological samples during analysis, leading to the interference of sample matrices. The absence of interference for the BIA-MPA simultaneous monitoring of UA and nitrite in

biological fluids was due to the short contact time of a microliter sample with the working electrode.¹²⁷

6. CONCLUSIONS

Screen-printing technology associated with injection techniques (FIA, SIA, and BIA) has attracted interest in several fields (pharmaceutical, industrial, clinical, environmental, etc.) and applications in real systems, ranging from natural waters, biofluids, (bio)fuels, and heavy metals, to name a few. All of the papers originating from the association of the flow techniques with screen-printed electrodes were brought together, starting from the first study performed in 2003 (quantification of lead on SPE), to the articles published until the end of 2020. In this period, analytical strategies based on electrochemical detection, especially amperometry and voltammetry, have been developed. In many cases, advanced procedures to successfully process very complex sample constituents for routine analysis have been reported. The tables presented along with the text demonstrated the variety of materials for modification of the SPEs (C, Au, Pt, Ag, metallic films, organic films, nanoparticles, carbon nanotubes, enzymes, etc.).

FIA presented the largest number of papers in the literature, mainly due to its longer time as an analytical tool for the mechanization of systems in comparison to the other techniques. The combination of FIA–SPE has received the most attention among the flow injection techniques, with over 60 manuscripts reported. Advantages associated with these techniques include high sample throughput, automation, repeatability, high sensitivity, sample handling capabilities, low reagent consumption, and waste generation. SPE based biosensors were mostly employed for the determination of glucose and NADH, but also for the screening of organophosphorus pesticides, UA, and lactate. BIA was the latest technique to be coupled with SPE. However, in order to compensate, in only 6 years of this association it has already surpassed the number of papers published in the SIA–SPE section, which can perhaps be attributed to its higher portability and simplicity for miniaturization. Although the first demonstration of BIA combined with SPE happened only half a decade ago, features such as simple instrumentation, high portability, and easy miniaturization have attracted interest in this approach, and electrochemical cells based on 3D printed technology have been reported and also made available commercially.

This revision also addresses a rapid overview on the evolution of the processes involved in the construction of the screen-printed electrodes. The availability of battery-powered potentiostats has facilitated the development of this portable arrangement, demonstrating great potential for point-of-care and on-site analysis, especially in developing countries. The analytical capabilities of these associations make them very attractive due to their simplicity, robustness, high-throughput capacity, and relatively low cost. The development of new materials will further increase the applicability of these setups for large-scale use and automation systems, opening many perspectives to extend it to other technologies (such as further miniaturization, paper SPE, and wearable devices), as well as in the diagnosis of infectious diseases (e.g., SARS-CoV-2, influenza, HPV, rubella, hepatitis, HIV/AIDS).

AUTHOR INFORMATION

Corresponding Authors

Nathália Florência Barros Azeredo – *Institute of Chemistry, University of São Paulo, São Paulo 05508-070, Brazil; Department of Nanoengineering, University of California San Diego, La Jolla, California 92093, United States;* orcid.org/0000-0002-8121-3643; Email: nathalia@iq.usp.br

Lúcio Angnes – *Institute of Chemistry, University of São Paulo, São Paulo 05508-070, Brazil;* Email: luangnes@iq.usp.br

Authors

Mauro S. Ferreira Santos – *Institute of Chemistry, University of São Paulo, São Paulo 05508-070, Brazil;* Present Address: NASA Jet Propulsion Laboratory, California Institute of Technology, Pasadena, CA 91109, USA

Juliane R. Sempionatto – *Department of Nanoengineering, University of California San Diego, La Jolla, California 92093, United States*

Joseph Wang – *Department of Nanoengineering, University of California San Diego, La Jolla, California 92093, United States;* orcid.org/0000-0002-4921-9674

Complete contact information is available at:

<https://pubs.acs.org/10.1021/acs.analchem.1c02637>

Notes

The authors declare no competing financial interest.

Biographies

Nathalia Florencia B. Azeredo received a Degree in Chemistry from State University in the Northern Rio de Janeiro (UENF) with an internship period abroad spent at the University of La Verne (2011) and a Master's Degree in Natural Sciences in the research topic of Coordination and Bioinorganic Chemistry at UENF (2016). She completed her Ph.D. at the Institute of Chemistry in the University of São Paulo (2021). While pursuing her Ph.D., she spent 14 months as a visiting Ph.D. scholar at the University of California in San Diego (Laboratory for Nanobioelectronics) under the supervision of Prof. Joseph Wang, with two scholarships from Capes: Sandwich Ph.D. (PDSE) and Training for Ph.D. students abroad (PrInt). She is currently a Postdoctoral researcher at the Institute for Energy and Nuclear Research (University of São Paulo), and her research interest involves the development of (nano)structured (bio)sensors and (bio)fuel cells and their respective applications.

Mauro S. Ferreira Santos is currently a technologist at the NASA Jet Propulsion Laboratory working on the development of analytical protocols and instrumentation focused on searching for life beyond Earth. He received his B.S. in Chemistry (2008) and a Specialization in Technological Chemistry (2010) from University Center FIEO – Brazil. In 2012 and 2016, he received his Master's and Ph.D. degrees in Chemistry (Analytical Chemistry) from University of São Paulo – Brazil, under the supervision of Prof. Dr. Ivano G. R. Gutz. While pursuing his Ph.D., he was a visiting student at The University of Texas at San Antonio (UTSA) and at Clemson University (2015–2016) under the supervision of Prof. Dr. Carlos D. Garcia. In 2018, he joined the Chemical Analysis and Life Detection group at NASA Jet Propulsion Laboratory as a postdoctoral researcher. His areas of interest are electroanalytical chemistry, separation science, microfluidic devices, analytical instrumentation, and astrobiology.

Juliane R. Sempionatto received her B.S. degree in chemistry from the University of Sao Paulo (USP), M.S. degree in Material Science from Sao Paulo State University (Unesp), Brazil, and Ph.D. degree in

Nanoengineering from the University of California, San Diego, under the supervision of Professor Joseph Wang. Her background experience ranges from electrochemistry, biosensors, analytical chemistry, advanced materials for sensing application, and flexible and stretchable electrodes. She is currently focusing on developing much needed noninvasive wearable electrochemical biosensors for real-life applications toward the prevention and monitoring of diseases. Her research has broadened the field of wearable sensors with her significant contribution and innovation. During her Ph.D., Juliane published more than 20 peer reviewed papers and received the prestigious Siebel 2021 scholar award. Juliane is currently a postdoctoral researcher at California Institute of Technology (Caltech) where she continues the work on electrochemical sensors for wearable health sensors under the supervision of Professor Wei Gao.

Joseph Wang is a Distinguished Professor, SAIC Endowed Chair, and former Chair of the Department of Nanoengineering at University of California, San Diego (UCSD). He is also the Director of the UCSD Center of Wearable Sensors and Co-Director of the UCSD Center of Mobile Health Systems and Applications (CMSA). He served as the director of Center for Bioelectronics and Biosensors of Arizona State University (ASU) before joining UCSD. Prof. Wang has published more than 1200 papers and 11 books and he holds 30 patents (H Index = 178, >132 000 citations). He received two American Chemical Society National Awards in 1999 (Instrumentation) and 2006 (Electrochemistry), ECS Sensor Achievement Award (2018), and five Honorary Professors from Spain, Argentina, Czech Republic, Romania, China, and Slovenia. Prof. Wang is a Founding Editor of *Electroanalysis* (Wiley) and is an RSC, ECS, and AIMBE Fellow and a Thomson Reuters Highly Cited Researcher. His scientific interests are concentrated in the areas of bioelectronics, wearable devices, biosensors, bionanotechnology, nanomachines and microrobots, flexible materials, and electroanalytical chemistry.

Lúcio Angnes is a full professor at the Institute of Chemistry of the University of Sao Paulo. His research interests include the construction of electrodes with new and alternative materials, development of modified electrodes, arrays of microelectrodes, the design of different procedures of enzyme immobilization, and association of the created devices with flowing systems (flow and batch injection analysis). He has authored more than 180 research papers, is a member of the scientific board of *Biosensors & Bioelectronics*, *Electroanalysis*, *Biosensors*, and *Journal of Pharmaceutical Research*, among others. He is a member of the Sao Paulo State Academy of Science.

ACKNOWLEDGMENTS

N.F.B. Azeredo is thankful to Coordenação de Aperfeiçoamento de Pessoal de Nível Superior (Capes/Proex) and also to CAPES/PDSE for the Sandwich Ph.D. scholarship (Process 88881.186873/2018-01). The support from the São Paulo State Research Foundation (FAPESP – process 2017/13137-5) and INCT/Fapesp (process 2014/50867-3) is acknowledged. L.A. thanks the fellowship from the National Council for Research (process 311847-2018-8).

ABBREVIATIONS

ACH, aluminum chlorohydrate; AChEi, anticholinesterase; ASV, adsorptive stripping voltammetry; BIA, batch injection analysis; CNF, carbon nanofibers; CHIT, chitosan; CNT, carbon nanotubes; CoPc, cobalt phthalocyanine; cry, cryogel; CV, cyclic voltammetry; DPV, differential pulse voltammetry; D μ FD, disposable microfluidic device; DPPH, 2,2-diphenyl-1-

picrylhydrazyl; FIA, flow injection analysis; GOx, glucose oxidase; AuNPs, gold nanoparticles; GO, graphene oxide; HPLC, high-performance liquid chromatography; H₂O₂, hydrogen peroxide; INZ, isoniazid; LOD, limit of detection; MO, malaoxon; MBRs, Meldola's Blue-Reinecke salt; MPA, multiple-pulse amperometry; NPs, nanoparticles; NMD, nimodipine; OIs, organophosphate insecticides; RSD, relative standard deviation; *S. tryphi*, *Salmonella typhimurium*; SPCE, screen-printed carbon electrodes; SPE, screen-printed electrode; SPAuE, screen-printed gold electrode; SIA, sequential injection analysis; SWASV, square-wave anodic stripping voltammetry; SWV, square wave voltammetry; UA, uric acid; ZPT, zinc pyrrithione

REFERENCES

- (1) Yang, J.; Wang, K.; Xu, H.; Yan, W.; Jin, Q.; Cui, D. *Talanta* **2019**, *202*, 96–110.
- (2) Yang, K.; Wu, J.; Santos, S.; Liu, Y.; Zhu, L.; Lin, F. *Biosens. Bioelectron.* **2019**, *124–125*, 150–160.
- (3) Lu, L. *Biosens. Bioelectron.* **2018**, *110*, 180–192.
- (4) Carvajal, M. A.; Ballesta-Claver, J.; Morales, D. P.; Palma, A. J.; Valencia-Mirón, M. C.; Capitán-Vallvey, L. F. *Sens. Actuators, B* **2012**, *169*, 46–53.
- (5) Li, M.; Li, Y.-T.; Li, D.-W.; Long, Y.-T. *Anal. Chim. Acta* **2012**, *734*, 31–44.
- (6) Li, M.; Li, D.-W.; Xiu, G.; Long, Y.-T. *Curr. Opin. Electrochem.* **2017**, *3* (1), 137–143.
- (7) Nascimento, V. B.; Angnes, L. *Quim. Nova* **1998**, *21* (5), 614–629.
- (8) Ružička, J.; Hansen, E. H. *Anal. Chim. Acta* **1974**, *69* (1), 129–141.
- (9) Ahmed, M. U.; Hossain, M. M.; Safavieh, M.; Wong, Y. L.; Rahman, I. A.; Zourob, M.; Tamiya, E. *Crit. Rev. Biotechnol.* **2016**, *36* (3), 495–505.
- (10) Ruzicka, J.; Marshall, G. D. *Anal. Chim. Acta* **1990**, *237*, 329–343.
- (11) Pimenta, A. M.; Montenegro, M. C. B. S. M.; Araújo, A. N.; Calatayud, J. M. J. *Pharm. Biomed. Anal.* **2006**, *40* (1), 16–34.
- (12) Wang, J.; Taha, Z. *Anal. Chem.* **1991**, *63* (10), 1053–1056.
- (13) Rocha, F. R. P.; Zagatto, E. A. G. *Talanta* **2020**, *206*, 120185.
- (14) Bezerra, M. A.; Lemos, V. A.; de Oliveira, D. M.; Novaes, C. G.; Barreto, J. A.; Alves, J. P. S.; Cerqueira, U. M. F. d. M.; Santos, Q. O. d.; Araújo, S. A. *Microchem. J.* **2020**, *155*, 104731.
- (15) Rocha, D. P.; Cardoso, R. M.; Tormin, T. F.; de Araujo, W. R.; Munoz, R. A. A.; Richter, E. M.; Angnes, L. *Electroanalysis* **2018**, *30* (7), 1386–1399.
- (16) García-Miranda Ferrari, A.; Rowley-Neale, S. J.; Banks, C. E. *Talanta Open* **2021**, *3*, 100032.
- (17) Squizzato, A. L.; Munoz, R. A. A.; Banks, C. E.; Richter, E. M. *ChemElectroChem* **2020**, *7* (10), 2211–2221.
- (18) Wikipedia, Screen Printing. https://en.wikipedia.org/wiki/Screen_printing (accessed Dec 2020).
- (19) Granado Rico, M. A.; Olivares-Marín, M.; Gil, E. P. *Electroanalysis* **2008**, *20* (24), 2608–2613.
- (20) Serrano, N.; Díaz-Cruz, J. M.; Ariño, C.; Esteban, M. *Electroanalysis* **2010**, *22* (13), 1460–1467.
- (21) Arduini, F.; Micheli, L.; Moscone, D.; Paleschi, G.; Piermarini, S.; Ricci, F.; Volpe, G. *TrAC, Trends Anal. Chem.* **2016**, *79*, 114–126.
- (22) Mohamed, H. M. *TrAC, Trends Anal. Chem.* **2016**, *82*, 1–11.
- (23) DropSens. Screen-printed electrodes. http://www.dropsens.com/en/screen_printed_electrodes_pag.html (accessed Jan 2021).
- (24) Schlisske, S.; Rosenauer, C.; Rödlmeier, T.; Giringner, K.; Michels, J. J.; Kremer, K.; Lemmer, U.; Morsbach, S.; Daoulas, K. C.; Hernandez-Sosa, G. *Adv. Mater. Technol.* **2021**, *6* (2), 2000335.
- (25) Youtube. The 99 cent ZP screen printed electrode. <https://www.youtube.com/watch?v=8JrN1yQJOYI> (accessed Jan 2021).

- (26) Fletcher, S. Screen-Printed Carbon Electrodes. In *Electrochemistry of Carbon Electrodes*; Alkire, R. C., Bartlett, P. N., Lipkowsky, J., Eds.; WileyVCH Verlag GmbH & Co. KGaA: Weinheim, Germany, 2020; pp 425–444.
- (27) Chang, W.-L.; Kumar, A. S.; Wang, S.-P.; Yang, C.-H.; Shih, Y. *Electrochim. Acta* **2016**, *195*, 199–207.
- (28) Ke, J.-H.; Tseng, H.-J.; Hsu, C.-T.; Chen, J.-C.; Muthuraman, G.; Zen, J.-M. *Sens. Actuators, B* **2008**, *130* (2), 614–619.
- (29) Neves, M. M. P. S.; González-García, M. B.; Hernández-Santos, D.; Fanjul-Bolado, P. *ChemElectroChem* **2017**, *4* (7), 1686–1689.
- (30) Kunpatee, K.; Chamsai, P.; Mehmeti, E.; Stankovic, D. M.; Ortner, A.; Kalcher, K.; Samphao, A. *J. Electroanal. Chem.* **2019**, *855*, 113630.
- (31) de Oliveira, T. R.; Martucci, D. H.; Faria, R. C. *Sens. Actuators, B* **2018**, *255*, 684–691.
- (32) Sue, J.-W.; Ku, H.-H.; Chung, H.-H.; Zen, J.-M. *Electrochem. Commun.* **2008**, *10* (7), 987–990.
- (33) Bergamini, M. F.; Santos, A. L.; Stradiotto, N. R.; Zanon, M. V. *B. J. Pharm. Biomed. Anal.* **2007**, *43* (1), 315–319.
- (34) Mozo, J. D.; Carbajo, J.; Sturm, J. C.; Núñez-Vergara, L. J.; Salgado, P.; Squella, J. A. *Electroanalysis* **2012**, *24* (3), 676–682.
- (35) Gopinathan, M.; Thiyagarajan, N.; Thirupathi, M.; Zen, J.-M. *Electroanalysis* **2018**, *30* (7), 1400–1406.
- (36) Carneiro, E. A.; Agustini, D.; Figueiredo-Filho, L. C. S.; Banks, C. E.; Marcolino-Junior, L. H.; Bergamini, M. F. *Electroanalysis* **2018**, *30* (1), 101–108.
- (37) Vandeput, M.; Rodríguez-Gómez, R.; Izere, A.-M.; Zafra-Gómez, A.; De Braekeleer, K.; Delporte, C.; Van Antwerpen, P.; Kauffmann, J.-M. *Electroanalysis* **2018**, *30* (7), 1293–1302.
- (38) Chiu, M.-H.; Yang, H.-H.; Liu, C.-H.; Zen, J.-M. *J. Chromatogr. B: Anal. Technol. Biomed. Life Sci.* **2009**, *877* (10), 991–994.
- (39) Hsu, C.-T.; Chung, H.-H.; Lyuu, H.-J.; Tsai, D.-M.; Kumar, A. S.; Zen, J.-M. *Anal. Sci.* **2006**, *22* (1), 35–38.
- (40) Němečková-Makrlíková, A.; Matysik, F.-M.; Navrátil, T.; Barek, J.; Vyskočil, V. *Electroanalysis* **2019**, *31* (2), 303–308.
- (41) Fanjul-Bolado, P.; Lamas-Ardisana, P. J.; Hernández-Santos, D.; Costa-García, A. *Anal. Chim. Acta* **2009**, *638* (2), 133–138.
- (42) Stefano, J. S.; Montes, R. H. O.; Richter, E. M.; Muñoz, R. A. A. *J. Braz. Chem. Soc.* **2014**, *25*, 484–491.
- (43) Ochiai, L. M.; Agustini, D.; Figueiredo-Filho, L. C. S.; Banks, C. E.; Marcolino-Junior, L. H.; Bergamini, M. F. *Sens. Actuators, B* **2017**, *241*, 978–984.
- (44) Salgado-Figueroa, P.; Gutiérrez, C.; Squella, J. A. *Sens. Actuators, B* **2015**, *220*, 456–462.
- (45) Salgado-Figueroa, P.; Jara-Ulloa, P.; Alvarez-Lueje, A.; Núñez-Vergara, L. J.; Squella, J. A. *J. Electrochem. Soc.* **2013**, *160* (9), H553–H559.
- (46) Reanpang, P.; Themsirimongkon, S.; Saipanya, S.; Chailapakul, O.; Jakmune, J. *Talanta* **2015**, *144*, 868–874.
- (47) Salgado-Figueroa, P.; Jara-Ulloa, P.; Alvarez-Lueje, A.; Squella, J. A. *Electroanalysis* **2013**, *25* (6), 1433–1438.
- (48) Upan, J.; Reanpang, P.; Chailapakul, O.; Jakmune, J. *Talanta* **2016**, *146*, 766–771.
- (49) Fonseca, S.; Caneppele, G. L.; Backes, R.; Ferreira, B. D.; da Silva, R. A. B.; Martins, C. A. *J. Electroanal. Chem.* **2017**, *789*, 38–43.
- (50) Masawat, P.; Liawruangrath, S.; Slater, J. M. *Sens. Actuators, B* **2003**, *91* (1), 52–59.
- (51) Delile, S.; Aussage, A.; Maillou, T.; Palmas, P.; Lair, V.; Cassir, M. *Talanta* **2015**, *132*, 334–338.
- (52) Shaidarova, L. G.; Chelnokova, I. A.; Il'ina, M. A.; Leksina, Y. A.; Budnikov, H. C. *J. Anal. Chem.* **2019**, *74* (6), 584–590.
- (53) Chiu, M.-H.; Kumar, A. S.; Sornambikai, S.; Zen, J.-M.; Shih, Y. *Electroanalysis* **2010**, *22* (20), 2421–2427.
- (54) Promsuwan, K.; Thavarungkul, P.; Kanatharana, P.; Limbut, W. *Electrochim. Acta* **2017**, *232*, 357–369.
- (55) Chen, P.-Y.; Yang, H.-H.; Huang, C.-C.; Chen, Y.-H.; Shih, Y. *Electrochim. Acta* **2015**, *161*, 100–107.
- (56) Salazar, P.; Rico, V.; González-Elipse, A. R. *Electroanalysis* **2018**, *30* (1), 187–193.
- (57) Henriquez, C.; Laglera, L. M.; Alpizar, M. J.; Calvo, J.; Arduini, F.; Cerdà, V. *Talanta* **2012**, *96*, 140–146.
- (58) Oliveira, P. R. d.; Oliveira, M. M.; Zarbin, A. J. G.; Marcolino-Junior, L. H.; Bergamini, M. F. *Sens. Actuators, B* **2012**, *171–172*, 795–802.
- (59) Nellaippan, S.; Kumar, A. S. *J. Electroanal. Chem.* **2017**, *801*, 171–178.
- (60) Shih, Y.; Zen, J.-M.; Kumar, A. S.; Chen, P.-Y. *Talanta* **2004**, *62* (5), 912–917.
- (61) Huayhuas-Chipana, B. C.; Foguel, M. V.; Gonçalves, L. M.; Sotomayor, M. D. P. T. *Microchem. J.* **2017**, *131*, 92–97.
- (62) Talarico, D.; Cinti, S.; Arduini, F.; Amine, A.; Moscone, D.; Palleschi, G. *Environ. Sci. Technol.* **2015**, *49* (13), 7934–7939.
- (63) Salazar, P.; Martín, M.; González-Mora, J. L.; González-Elipse, A. R. *Talanta* **2016**, *146*, 410–416.
- (64) Punrat, E.; Maksuk, C.; Chuanuwatanakul, S.; Wonsawat, W.; Chailapakul, O. *Talanta* **2016**, *150*, 198–205.
- (65) Huang, C.-Y.; O'Hare, D.; Chao, I. J.; Wei, H.-W.; Liang, Y.-F.; Liu, B.-D.; Lee, M.-H.; Lin, H.-Y. *Biosens. Bioelectron.* **2015**, *67*, 208–213.
- (66) Chen, Y.-J.; Chang, J.-L.; Thiyagarajan, N.; Zen, J.-M. *Electrocatalysis* **2018**, *9* (4), 444–451.
- (67) Smart, A.; Crew, A.; Pemberton, R.; Hughes, G.; Doran, O.; Hart, J. P. *TrAC, Trends Anal. Chem.* **2020**, *127*, 115898.
- (68) Turkusic, E.; Kalcher, K.; Kahrovic, E.; Beyene, N. W.; Moderegger, H.; Sofic, E.; Begic, S.; Kalcher, K. *Talanta* **2005**, *65* (2), 559–564.
- (69) Samphao, A.; Butmee, P.; Jitcharoen, J.; Švorc, Č.; Raber, G.; Kalcher, K. *Talanta* **2015**, *142*, 35–42.
- (70) Liu, J.; Sun, S.; Liu, C.; Wei, S. *Measurement* **2011**, *44* (10), 1878–1883.
- (71) Piano, M.; Serban, S.; Biddle, N.; Pittson, R.; Drago, G. A.; Hart, J. P. *Anal. Biochem.* **2010**, *396* (2), 269–274.
- (72) Sun, C.-L.; Cheng, W.-L.; Hsu, T.-K.; Chang, C.-W.; Chang, J.-L.; Zen, J.-M. *Electrochem. Commun.* **2013**, *30*, 91–94.
- (73) Shi, M.; Xu, J.; Zhang, S.; Liu, B.; Kong, J. *Talanta* **2006**, *68* (4), 1089–1095.
- (74) Dominguez, R. B.; Alonso, G. A.; Muñoz, R.; Hayat, A.; Marty, J.-L. *Sens. Actuators, B* **2015**, *208*, 491–496.
- (75) Arduini, F.; Neagu, D.; Scognamiglio, V.; Patarino, S.; Moscone, D.; Palleschi, G. *Chemosensors* **2015**, *3* (2), 129–145.
- (76) Du, D.; Wang, J.; Smith, J. N.; Timchalk, C.; Lin, Y. *Anal. Chem.* **2009**, *81* (22), 9314–9320.
- (77) Mishra, R. K.; Alonso, G. A.; Istamboulie, G.; Bhand, S.; Marty, J.-L. *Sens. Actuators, B* **2015**, *208*, 228–237.
- (78) Chekin, F.; Gorton, L.; Tapsoba, I. *Anal. Bioanal. Chem.* **2015**, *407* (2), 439–446.
- (79) Lanzelotto, C.; Favero, G.; Antonelli, M. L.; Tortolini, C.; Cannistraro, S.; Coppari, E.; Mazzei, F. *Biosens. Bioelectron.* **2014**, *55*, 430–437.
- (80) Caetano, F. R.; Carneiro, E. A.; Agustini, D.; Figueiredo-Filho, L. C. S.; Banks, C. E.; Bergamini, M. F.; Marcolino-Junior, L. H. *Biosens. Bioelectron.* **2018**, *99*, 382–388.
- (81) Frangu, A.; Pravcová, K.; Šilarová, P.; Arbnesi, T.; Sýs, M. *Anal. Bioanal. Chem.* **2019**, *411* (11), 2415–2424.
- (82) Gao, Q.; Cui, X.; Yang, F.; Ma, Y.; Yang, X. *Biosens. Bioelectron.* **2003**, *19* (3), 277–282.
- (83) Gao, Q.; Wang, W.; Ma, Y.; Yang, X. *Talanta* **2004**, *62* (3), 477–482.
- (84) Piano, M.; Serban, S.; Pittson, R.; Drago, G. A.; Hart, J. P. *Talanta* **2010**, *82* (1), 34–37.
- (85) Gao, Q.; Ma, Y.; Cheng, Z.; Wang, W.; Yang, X. *Anal. Chim. Acta* **2003**, *488* (1), 61–70.
- (86) Biscay, J.; González García, M. B.; Costa García, A. *Talanta* **2015**, *131*, 706–711.
- (87) Rhouati, A.; Hayat, A.; Hernandez, D. B.; Meraihi, Z.; Munoz, R.; Marty, J.-L. *Sens. Actuators, B* **2013**, *176*, 1160–1166.

- (88) Kurbanoglu, S.; Mayorga-Martinez, C. C.; Medina-Sánchez, M.; Rivas, L.; Ozkan, S. A.; Merkoçi, A. *Biosens. Bioelectron.* **2015**, *67*, 670–676.
- (89) da Cruz, F. S.; Paula, F. d. S.; Franco, D. L.; dos Santos, W. T. P.; Ferreira, L. F. J. *Electroanal. Chem.* **2017**, *806*, 172–179.
- (90) Jirakunakorn, R.; Khumngern, S.; Choosang, J.; Thavarungkul, P.; Kanatharana, P.; Numnuam, A. *Microchem. J.* **2020**, *154*, 104624.
- (91) Pérez-Olmos, R.; Soto, J. C.; Zárate, N.; Araújo, A. N.; Montenegro, M. C. B. S. M. *Anal. Chim. Acta* **2005**, *554* (1), 1–16.
- (92) Guzsány, V.; Nakajima, H.; Soh, N.; Nakano, K.; Imato, T. *Anal. Chim. Acta* **2010**, *658* (1), 12–17.
- (93) Ninwong, B.; Chuanuwatanakul, S.; Chailapakul, O.; Dungchai, W.; Motomizu, S. *Talanta* **2012**, *96*, 75–81.
- (94) Injang, U.; Noyrod, P.; Siangproh, W.; Dungchai, W.; Motomizu, S.; Chailapakul, O. *Anal. Chim. Acta* **2010**, *668* (1), 54–60.
- (95) Keawkim, K.; Chuanuwatanakul, S.; Chailapakul, O.; Motomizu, S. *Food Control* **2013**, *31* (1), 14–21.
- (96) Chiu, M.-H.; Wu, H.; Chen, J.-C.; Muthuraman, G.; Zen, J.-M. *Electroanalysis* **2007**, *19* (22), 2301–2306.
- (97) Punrat, E.; Chuanuwatanakul, S.; Kaneta, T.; Motomizu, S.; Chailapakul, O. *Talanta* **2013**, *116*, 1018–1025.
- (98) Nascimento, F. H. d.; Masini, J. C. *Quim. Nova* **2017**, *41*, 43–48.
- (99) do Nascimento, F. H.; Masini, J. C. *Talanta* **2012**, *100*, 57–63.
- (100) Punrat, E.; Chuanuwatanakul, S.; Kaneta, T.; Motomizu, S.; Chailapakul, O. *J. Electroanal. Chem.* **2014**, *727*, 78–83.
- (101) Ribeiro, L. F.; Masini, J. C. *Electroanalysis* **2014**, *26* (12), 2754–2763.
- (102) Ruengpirasiri, P.; Punrat, E.; Chailapakul, O.; Chuanuwatanakul, S. *Electroanalysis* **2017**, *29* (4), 1022–1030.
- (103) Chuntib, P.; Themsirimongkon, S.; Saipanya, S.; Jakmunee, J. *Talanta* **2017**, *170*, 1–8.
- (104) Thunkhamrak, C.; Reanpang, P.; Ounnunkad, K.; Jakmunee, J. *Talanta* **2017**, *171*, 53–60.
- (105) Veloso, W. B.; Ribeiro, G. A. C.; da Rocha, C. Q.; Tanaka, A. A.; da Silva, I. S.; Dantas, L. M. F. *Measurement* **2020**, *155*, 107516.
- (106) Alexovič, M.; Horstkotte, B.; Šrámková, I.; Solich, P.; Sabo, J. *TrAC, Trends Anal. Chem.* **2017**, *86*, 39–55.
- (107) Ferreira, L. M. C.; Felix, F. S.; Angnes, L. *Electroanalysis* **2012**, *24* (4), 961–966.
- (108) Tormin, T. F.; Cunha, R. R.; da Silva, R. A. B.; Munoz, R. A. A.; Richter, E. M. *Sens. Actuators, B* **2014**, *202*, 93–98.
- (109) Hernández-Santos, D.; Fanjul-Bolado, P.; González-García, M. B. Batch injection analysis for amperometric determination of ascorbic acid at ruthenium dioxide screen-printed electrodes. In *Laboratory Methods in Dynamic Electroanalysis*; Fernandez Abedul, M. T., Ed.; Elsevier, 2020; pp 99–108.
- (110) Correa, A. L.; Gonçalves, J. M.; Rossini, P. O.; Bernardes, J. S.; Neves, C. A.; Araki, K.; Angnes, L. *Talanta* **2018**, *186*, 354–361.
- (111) Cardoso, R. M.; Kalinke, C.; Rocha, R. G.; dos Santos, P. L.; Rocha, D. P.; Oliveira, P. R.; Janegitz, B. C.; Bonacin, J. A.; Richter, E. M.; Munoz, R. A. A. *Anal. Chim. Acta* **2020**, *1118*, 73–91.
- (112) Youtube. Biaspe cell - a portable electrochemical system for on-site analysis. <https://www.youtube.com/watch?v=IaPjMZrojpu> and https://www.youtube.com/watch?v=oe0G2RA_t4o (accessed Dec 2020).
- (113) Richter, E. M.; Tormin, T. F.; Cunha, R. R.; Silva, W. P.; Pérez-Junquera, A.; Fanjul-Bolado, P.; Hernández-Santos, D.; Muñoz, R. A. A. *Electroanalysis* **2016**, *28* (8), 1856–1859.
- (114) Ribeiro, G. A. C.; da Rocha, C. Q.; Veloso, W. B.; Fernandes, R. N.; da Silva, I. S.; Tanaka, A. A. *Microchem. J.* **2019**, *146*, 1249–1254.
- (115) Caramit, R. P.; Lucca, B. G.; Souza Ferreira, V.; Abarza Munoz, R. A.; Richter, E. M.; da Silva, R. A. B. *Electroanalysis* **2015**, *27* (2), 271–275.
- (116) Almeida, E. S.; Silva, L. A. J.; Sousa, R. M. F.; Richter, E. M.; Foster, C. W.; Banks, C. E.; Munoz, R. A. A. *Anal. Chim. Acta* **2016**, *934*, 1–8.
- (117) Almeida, E. S.; Richter, E. M.; Munoz, R. A. A. *Electroanalysis* **2016**, *28* (3), 633–639.
- (118) Squizzato, A. L.; Silva, W. P.; Del Claro, A. T. S.; Rocha, D. P.; Dornellas, R. M.; Richter, E. M.; Foster, C. W.; Banks, C. E.; Munoz, R. A. A. *Talanta* **2017**, *174*, 420–427.
- (119) Arantes, I. V. S.; Stefano, J. S.; Sousa, R. M. F.; Richter, E. M.; Foster, C. W.; Banks, C. E.; Muñoz, R. A. A. *Electroanalysis* **2018**, *30* (6), 1192–1197.
- (120) Stefano, J. S.; Dias, A. C.; Arantes, I. V. S.; Costa, B. M. C.; Silva, L. A. J.; Richter, E. M.; Banks, C. E.; Munoz, R. A. A. *Electroanalysis* **2018**, *31* (3), 518–526.
- (121) Tormin, T. F.; Oliveira, G. K. F.; Richter, E. M.; Munoz, R. A. A. *Electroanalysis* **2016**, *28* (5), 940–946.
- (122) Stefano, J. S.; Tormin, T. F.; da Silva, J. P.; Richter, E. M.; Munoz, R. A. A. *Microchem. J.* **2017**, *133*, 398–403.
- (123) Stefano, J. S.; Cordeiro, D. S.; Marra, M. C.; Richter, E. M.; Munoz, R. A. A. *Electroanalysis* **2016**, *28* (2), 350–357.
- (124) de Lima, R. M. F.; de Oliveira Silva, M. D.; Felix, F. S.; Angnes, L.; dos Santos, W. T. P.; Saczk, A. A. *Electroanalysis* **2018**, *30* (2), 283–287.
- (125) Freitas, H. C.; Almeida, E. S.; Tormin, T. F.; Richter, E. M.; Munoz, R. A. A. *Anal. Methods* **2015**, *7* (17), 7170–7176.
- (126) Dias, A. A.; Cardoso, T. M. G.; Cardoso, R. M.; Duarte, L. C.; Muñoz, R. A. A.; Richter, E. M.; Coltro, W. K. T. *Sens. Actuators, B* **2016**, *226*, 196–203.
- (127) Caetano, L. P.; Lima, A. P.; Tormin, T. F.; Richter, E. M.; Espindola, F. S.; Botelho, F. V.; Munoz, R. A. A. *Electroanalysis* **2018**, *30* (8), 1870–1879.
- (128) Cardoso, R. M.; Mendonça, D. M. H.; Silva, W. P.; Silva, M. N. T.; Nossol, E.; da Silva, R. A. B.; Richter, E. M.; Muñoz, R. A. A. *Anal. Chim. Acta* **2018**, *1033*, 49–57.